

University of South Bohemia in České Budějovice

Faculty of Science

**The role of Q tRNA modification in codon biased translation in
*Leishmania mexicana***

Master thesis

Bc. Monika Švábová

Supervisor: RNDr. Zdeněk Paris, Ph. D.

Co-Supervisor: Sneha Kulkarni, Ph.D.

České Budějovice, 2022

Švábová, M., 2022: The role of Q tRNA modification in codon biased translation in *Leishmania mexicana*. Mgr. Thesis, in English – 62 p, Faculty of Science, University of South Bohemia, České Budějovice, Czech Republic.

Annotation

The aim of the thesis was to standardize polysome profiling and ribosome profiling protocols for the parasitic protist *Leishmania mexicana* in order to identify the effect of Q-tRNAs in translation. In addition, we analyzed the role of queuosine (Q) t-RNA modification in the cell cycle of *L. mexicana*. The proteomics analysis was carried out in order to elucidate the role of Q-tRNAs in protein folding.

Prohlášení (affirmation)

Prohlašuji, že jsem autorem této kvalifikační práce a že jsem ji vypracovala pouze s použitím pramenů a literatury uvedených v seznamu použitých zdrojů.

České Budějovice, 13th April 2022

.....
Monika Švábová

Acknowledgements

I would like to thank to my supervisor Zdeněk Paris for the opportunity to be part of his great team, to work in his laboratory and to participate in this project.

I am most grateful to my co-supervisor Sneha Kulkarni for introducing me to the world of RNA and its modifications and getting acquainted with *Leishmania mexicana*. Moreover, I also thank her for her valuable advice as well as for the time she spent supervising me and explaining the various intricacies of the research. Additionally, she taught me a remarkable number of molecular biology methods, helped me plan the timing of each experiment and patiently answered all my questions day and night.

My special thanks to all members of our lab for creating very pleasant and friendly atmosphere, namely Bankatesh, Eva H, Eva M, Veru and past member Helmut as well as all members of surrounding labs.

I would also like to thank to Julius Lukeš for allowing me to use the laboratory equipment in his lab.

Many thanks to Ondřej Gahura for the assistance and training in the use of ultracentrifuge and gradient station.

Finally, I must thank to my family for their moral support throughout all the years of my studies.

This work was supported by Czech Science Foundations grants (20-11585S to Zdeněk Paris). This work was also supported by ERDF/ESF project Centre for research of pathogenicity and virulence of parasites r.n.: CZ.02.1.01/0.0/0.0/16_019/0000759, funded by the European Regional Development Fund (ERDF) and the Ministry of Education, Youth and Sport, Czech Republic.

Table of content

1	Introduction	1
1.1	<i>Leishmania</i> & leishmaniasis	1
1.2	<i>Leishmania mexicana</i> life cycle	2
1.3	Types & functions of RNA	4
1.4	Processing & modifications of tRNA	4
1.5	Queuosine modification of tRNA (Q-tRNAs)	8
1.5.1	Queuosine	8
1.5.2	tRNA-guanine transglycosylase (TGT)	9
1.5.3	Role of Q-tRNAs in physiology	11
1.6	Codon biased translation	11
1.7	Queuosine modification in <i>Trypanosoma brucei</i>	14
1.8	Rationale of the project	15
2	Aims of the thesis	17
3	Materials and methods	18
3.1	Cell culture	18
3.2	Isolation of RNA	18
3.3	Boronate affinity electrophoresis and northern blotting	19
3.4	Oligonucleotide hybridization	19
3.5	Pulse labelling of proteins	20
3.6	Analysis of protein synthesis	20
3.7	Analysis of protein aggregates	20
3.8	Polysome isolation	21
3.8.1	Cell lysis	21
3.8.2	Polysome recovery	21
3.9	Ribosome profiling	22
3.9.1	Cell lysis	22

3.9.2	RNase digestion and ribosome recovery	22
3.9.3	RNA isolation from sucrose fractions	22
3.9.4	Footprint size selection	23
3.9.5	3' dephosphorylation	23
3.9.6	3' adaptor ligation	24
3.9.7	Reverse transcription (RT)	24
3.10	Flow cytometry	25
3.10.1	PI staining	25
3.10.2	TMRE staining	25
4	Results	27
4.1	Evaluation of the presence of Q in Lmx tRNA ^{Asp, His, Tyr}	27
4.2	Q modification does not affect the growth of <i>L. mexicana</i> in axenic culture	27
4.3	Q modification does not affect the cell cycle of <i>L. mexicana</i>	28
4.4	Q modification does not affect the mitochondrial membrane potential of <i>L. mexicana</i> procyclic promastigotes	30
4.5	Polysome analysis	31
4.5.1	Standardization	31
4.5.2	Standardized polysome profile for <i>L. mexicana</i>	33
4.5.3	Polysome analysis shows a role of Q-depletion in translation	34
4.5.4	Monosome density	35
4.6	Ribosome profiling	36
4.6.1	Standardization of RNase digestion	36
4.6.2	Standardized profiles of RNase digestion	37
4.6.3	Footprint size selection	38
4.6.4	Reverse transcription	39
4.7	Lack of Q can affect the rate of protein synthesis	39
4.8	Analysis of protein aggregates	40

5	Discussion	42
5.1	The presence of Q in Lmx tRNA ^{Asp, His, Tyr}	42
5.2	The effect of Q on cell growth, life cycle and membrane potential	42
5.3	Standardization of polysome profiling and ribosome profiling methods	43
5.4	Protein analysis	44
6	Conclusion	46
7	Appendix	47
7.1	Annex 1 – Common buffers	47
7.2	Annex 2 – Northern blotting and oligonucleotide hybridization buffers	49
7.3	Annex 3 – Proteomics buffers	51
7.4	Annex 4 – Oligonucleotide sequences	52
7.5	Annex 5 – RNA gel solutions	53
8	List of references	54

List of abbreviations

AA	<u>a</u> mino <u>a</u> cid
AB	<u>a</u> dd <u>b</u> ack
ADAT	tRNA-dependent adenosine deaminase
APB	3-(<u>a</u> crylamido)phenyl <u>b</u> oronic acid
APS	<u>a</u> mmonium <u>p</u> ersulfate
ATP	<u>a</u> denosine <u>t</u> riphosphate
BH4	tetrahydrobiopterin
bTGT	<u>b</u> acterial TGT
cDNA	<u>c</u> omplementary DNA
CL	<u>c</u> utaneous <u>l</u> eishmaniasis
DNA	<u>d</u> eoxyribo <u>n</u> ucleic <u>a</u> cid
dNTP	<u>d</u> eoxynu <u>c</u> leotide <u>t</u> riphosphate
DTT	<u>d</u> ithio <u>t</u> hreitol
e.g.	<i>exempli gratia</i>
EtBr	<u>e</u> thidium <u>b</u> romide
eTGT	<u>e</u> karyotic TGT
EtOH	<u>e</u> thyl alcohol
FBS	<u>f</u> etal <u>b</u> ovine <u>s</u> erum
FCCP	carbonyl cyanide- <i>p</i> -trifluoromethoxyphenylhydrazine
G	<u>g</u> uanosine
Hyg	<u>h</u> ygromycin
CHX	<u>c</u> yclo <u>h</u> eximide
IAA	<u>i</u> so <u>a</u> myl <u>a</u> lcohol
IGEPAL	octylphenoxypolyethocyethanol
KO	<u>k</u> nock- <u>o</u> ut
Lmx	<i>Leishmania m<u>e</u>xicana</i>

MCL	<u>m</u> uco <u>c</u> utaneous <u>l</u> eishmaniasis
MMP	<u>m</u> itochondrial <u>m</u> embrane <u>p</u> otential
mRNA	<u>m</u> essenger RNA
NaOH	sodium hydroxide
NP ₄₀	<u>n</u> onyl <u>p</u> henoxypolyethoxylethanol
nt	<u>n</u> ucleo <u>t</u> ide
Ntc	<u>n</u> ourseo <u>t</u> hricin
OD	<u>o</u> ptical <u>d</u> ensity
OX	periodate <u>o</u> xidized
PAA	poly <u>a</u> cryl <u>a</u> mid <u>e</u>
PAH	phenylalanine <u>h</u> ydroxylase
PBS	phosphate- <u>b</u> uffered <u>s</u> aline
Phleo	<u>p</u> hleomycin
PI	propidium <u>i</u> odide
PKDL	post- <u>k</u> ala-azar <u>d</u> ermal <u>l</u> eishmaniasis
PNK	polynucleotide <u>k</u> inase
Puro	<u>p</u> uromycin
Q	queuosine
q	queuine
QTRT1	queuine tRNA <u>r</u> ibo <u>t</u> ransferase <u>1</u>
QTRTD1	queuine tRNA <u>r</u> ibo <u>t</u> ransferase <u>d</u> omain containing <u>1</u>
RNA	<u>r</u> ibo <u>n</u> ucleic <u>a</u> cid
RPM	<u>r</u> evolutions per <u>m</u> inute
rRNA	<u>r</u> ibosomal RNA
RT	<u>r</u> everse <u>t</u> ranscription
SDS-PAGE	<u>s</u> odium <u>d</u> odecyl <u>s</u> ulfate- <u>p</u> oly <u>a</u> cryl <u>a</u> mid <u>e</u> <u>g</u> el <u>e</u> lectrophoresis
TAE	tris base/ <u>a</u> cetic acid/ <u>E</u> DTA

TEMED	<u>t</u> etramethylethylendi <u>a</u> min
TGT	<u>t</u> RNA-guanine <u>t</u> ransglycosylase
TMRE	<u>t</u> etramethyl <u>r</u> hodamine <u>e</u> thyl ester
Triton X-100	<i>t</i> -Octylphenoxypolyethoxyethanol
tRNA	<u>t</u> ransfer RNA
TRNT1	<u>t</u> RNA <u>n</u> ucleotidyl <u>t</u> ransferase <u>1</u>
Um	tRNA-dependent <u>u</u> ridine <u>m</u> ethyltransferase
VL	<u>v</u> isceral <u>l</u> eishmaniasis
WHO	<u>W</u> orld <u>H</u> ealth <u>O</u> rganization
WT	<u>w</u> ild type

1 Introduction

1.1 *Leishmania* & leishmaniasis

Leishmania, the genus of unicellular protozoan parasites, belongs to the kingdom Protista, order Trypanosomatida, and class Kinetoplastida. There are currently 53 *Leishmania* species identified, 31 of which are pathogenic to mammals and 20 to humans, causing a disease called leishmaniasis (Akhoundi et al., 2016). The species can be divided into two groups: the Old World species (*L. major*, *L. infantum*, and *L. tropica*) and New World species (*L. amazonensis*, *L. chagasi*, *L. mexicana*, *L. naiffi*, *L. braziliensis*, and *L. guyanensis*). Leishmaniasis is a vector-borne disease. Parasites are transmitted between vertebrates by the bite of infected female sandflies, mainly belonging to the genera *Phlebotomus* and *Lutzomyia* (de Vries et al., 2015). There are four types of the clinical manifestation of leishmaniasis depending on the *Leishmania* species, vector biology, and host factors – visceral leishmaniasis (VL, also known as kala-azar), post-kala-azar dermal leishmaniasis (PKDL), cutaneous leishmaniasis (CL), and mucocutaneous leishmaniasis (MCL) (Torres-Guerrero et al., 2017). According to WHO, the prevalence is 12 million cases with 30 000 new cases of VL and more than 1 million new cases of CL reported annually. However, most infected people may be asymptomatic. Additionally, there are many major risk factors. The most affected by leishmaniasis are poor, malnourished people with a weak immune system and lack of financial resources living in places where the population has been displaced. Moreover, climate change can also be a risk. Therefore, leishmaniasis is classified as a neglected disease that is included in supporting national control programs to prevent or control the disease (WHO 2021).

The most severe form is VL, usually caused by *L. donovani* and *L. infantum*. The mortality rate without treatment is over 95%. The symptoms are fever, weight loss, anemia, and enlargement of the spleen and liver. MCL is the most disabling form of the disease caused mainly by *L. braziliensis* and *L. panamensis*. It is manifested by the destruction of mucous membranes of the throat, mouth, and nose (Karamysheva et al., 2020). The most prevalent is the CL form, endemic in all subtropical and tropical areas (Asia, Africa, the Americas, and the Mediterranean region) (Fig. 1). This form is caused by both Old and New World *Leishmania* species, and the manifestations are skin lesions, mainly ulcers (Torres-Guerrero et al., 2017).

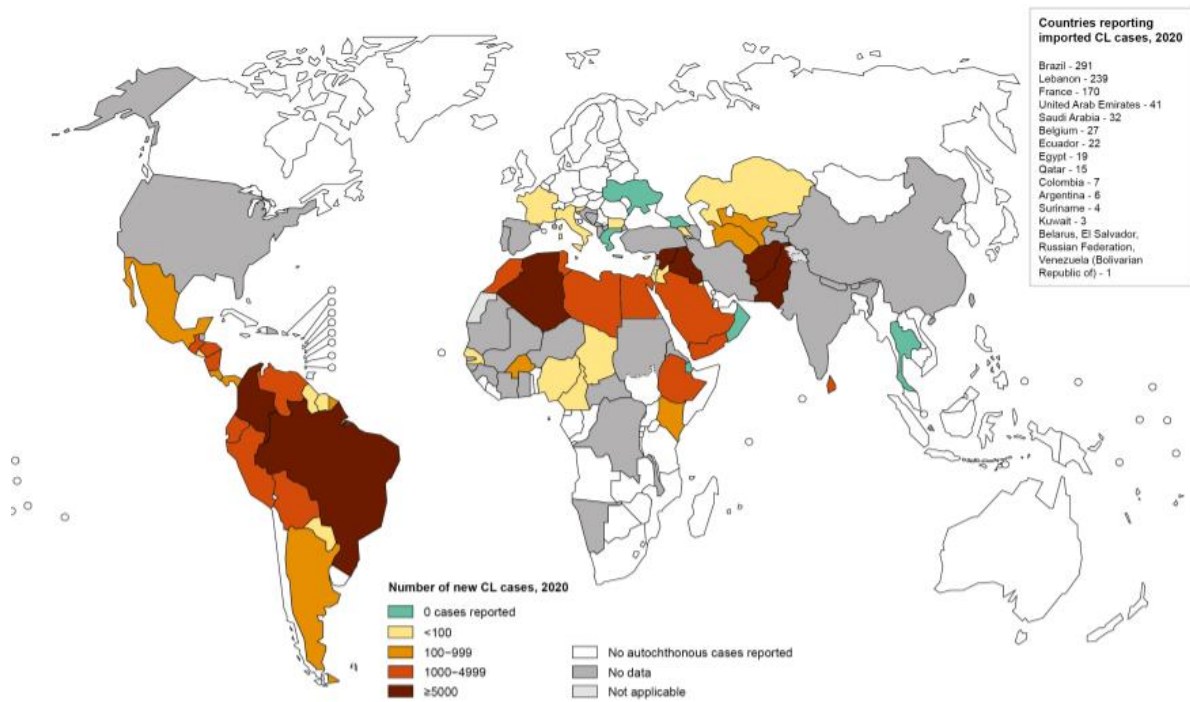


Fig. 1: Status of endemicity of cutaneous leishmaniasis (CL) worldwide, 2020 (WHO 2021).

Regarding treatment, there is currently chemotherapy with antimonials for CL and MCL forms, and Amphotericin B for VL. Unfortunately, these options exhibit many side effects, toxicity, and, in addition, the main problem is drug resistance. Currently, there is no approved vaccine against leishmaniasis (Taslimi et al., 2018).

1.2 *Leishmania mexicana* life cycle

Leishmania is an organism with a digenetic life cycle. The first stage, the extracellular flagellated promastigotes, is present in the sandfly vector, and the second stage, the intracellular non-flagellated amastigotes, is present in the mammalian host (McGwire & Satoskar, 2014).

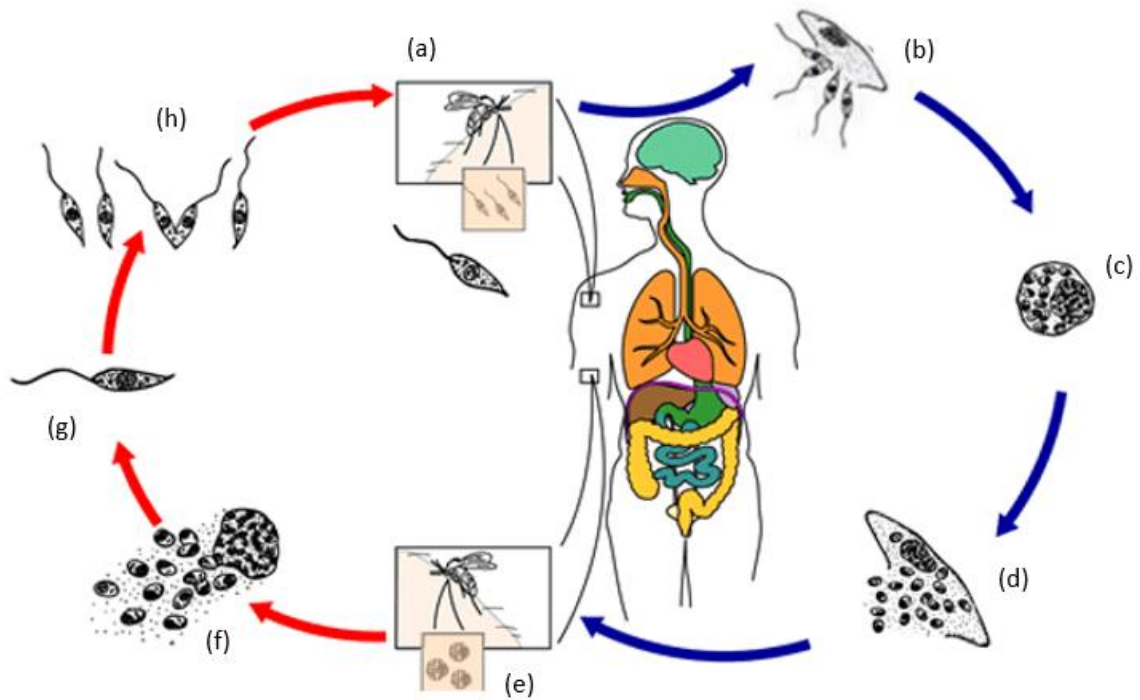


Fig. 2: *Leishmania* life cycle; (a) the infected female sand fly is taking a blood meal, and *Leishmania* promastigotes are transmitted into the skin of the mammalian host with the sand fly saliva; (b) promastigotes are phagocytosed by mononuclear phagocyte cells; (c) inside the host cells, the promastigotes are transformed into the amastigote stage; (d) the host cell full of amastigotes ruptures and released amastigotes infect other phagocytes; (e) another sand fly is taking a blood meal; (f, g, h) the amastigotes are transformed into procyclic promastigotes in the sand fly gut (modified from CDC, 2020).

The *Leishmania* life cycle is initiated by procyclic promastigotes that develop in the anterior midgut of the female *Phlebotomus*, where they survive and proliferate. Subsequently, they mature into the mammalian infective metacyclic forms, which takes approximately 4-5 days. The metacyclics must overcome many barriers to infect the sand fly. These barriers include digestive proteases, peritrophic membrane, digested blood meal excretion, and midgut structure and physiology. Following the maturation, the metacyclics migrate via intestines into the oesophagus. The *Leishmania* parasites are then transmitted into the skin of the mammalian host with the sand fly saliva during blood meals. The mononuclear phagocyte cells, including macrophages, monocytes, dendritic, and Langerhans cells, are chemoattracted to the area of the skin damaged by the bite, and many of the metacyclic promastigotes are phagocytosed by them and destroyed within newly formed phagolysosomes. Nevertheless, some of them survive and modify the phagolysosome into an acidic intracellular compartment, the parasitophorous vacuole in the host cell. Once inside this organelle, the promastigotes transform into the amastigote stage, which multiplies by binary fission. The host cell full of amastigotes may either become apoptotic or rupture. The apoptotic cells' amastigotes are taken over by other un-infected phagocytes, The amastigotes are released by cell lysis and may infect other mononuclear phagocytes that can metastasize within the skin or organs. Finally, when

another sand fly takes a blood meal, the amastigotes are transformed into procyclic promastigotes in the sand fly gut, completing the *Leishmania* life cycle (Fig. 2) (Gossage et al., 2003; Ramalho-Ortigao, 2010; Sacks & Kamhawi, 2001; Sunter & Gull, 2017).

1.3 Types & functions of RNA

Ribonucleic acid (RNA) is a single-stranded biopolymer composed of a strand of ribonucleotides containing phosphate groups and ribose sugars. The ribose alternates with a phosphate group that is covalently linked by a phosphodiester bond. The nitrogenous bases, adenine, guanine, cytosine, and uracil are attached to the ribose and represent units of inheritance. These nucleotides are involved in various biological processes, including coding, decoding, and the regulation of gene expression. There are three main types of RNA, which are the most studied and present in all organisms: messenger RNA (mRNA), ribosomal RNA (rRNA), and transfer RNA (tRNA).

Messenger RNA (mRNA) is formed by transcription according to the DNA template. Subsequently, it is read by the ribosome as a template for protein synthesis in the translation process.

Ribosomal RNA (rRNA) is the most common RNA molecule in a cell and it is transcribed in the nucleolus. rRNA is involved in a structural function of the ribosome along with specific proteins, and the catalytic activity of the ribosome. There are three differently sized rRNAs in prokaryotic organisms (23S, 16S, and 5S), in eukaryotic cells up to 4 types of rRNAs (28S, 18S, 5.8S, and 5S).

Transfer RNA (tRNA) is a type of RNA that participates in proteosynthesis by attaching a specific amino acid to a polypeptide chain, thereby translating mRNA into proteins (King et al., 2007; Wang & Farhana, 2022). This thesis focuses on tRNAs.

1.4 Processing & modifications of tRNA

tRNA, a special subtype of non-coding RNA encoded in the nucleus by RNA polymerase III, is a relatively small molecule containing 73 to 95 ribonucleotide residues, however, its significance in the translation process, in which proteins are formed according to the mRNA, is considerable. Moreover, tRNAs are involved in many other processes such as cell signaling, survival or apoptosis (Anderson & Ivanov, 2014).

Structurally, tRNAs may be described at three levels:

- i) Primary, determined by the nucleotide sequence
- ii) Secondary, formed by the interactions in the molecule and visualized as the cloverleaf structure
- iii) Tertiary structure with the three-dimensional disposition of the molecule, all tRNAs have identical basic L-shaped tertiary structures required for translation (Ouellette & Rawn, 2018).

Additionally, each tRNA molecule consist following parts: the T-arm, which contains a ribothymidine sequence (T ψ C, ψ = pseudouridine); the D-arm whose loop often contains dihydrouridine (DHU); the anticodon stem-loop with anticodon position represented by bases 34, 35 and 36; and the acceptor stem with a 5'-terminal phosphate group which contains a discriminator base (nucleotide 73), which is critical for charging and a conserved post-transcriptionally added CCA tail, (where amino acid is covalently bonded to the 3'-hydroxyl group). In addition, some tRNA molecules have a variable arm. Each arm is therefore composed of a double-stranded stem and single-stranded loop (Fig. 3) (Berg et al., 2019). Functionally, the two most important areas for the process of translation include the 3' acceptor stem - the region for attaching a specific amino acid (AA) - and the anticodon stem, which is a trinucleotide region recognizing the complementary bases of the mRNA. During translation, each tRNA transfers its specific AA, which is added to the growing polypeptide chain (Attardi, 1967).

The synthesis of tRNAs begins with the transcription of precursor molecules (pre-tRNAs) in the nucleus. Subsequently, the pre-tRNAs are subject to several alterations before their maturation. These maturation processes can be divided into i) early processes that include the removal of the 5' leader by RNase P and 3' trailer by RNase Z and ii) late processes in which a CAA tail is added to the 3' terminus by tRNA nucleotidyl transferase 1 (TRNT1). tRNAs are then aminoacylated and exported into the cytoplasm. In addition, some pre-tRNAs undergo intron removal as part of early processes (Phizicky & Hopper, 2015; Schaffer et al., 2019).

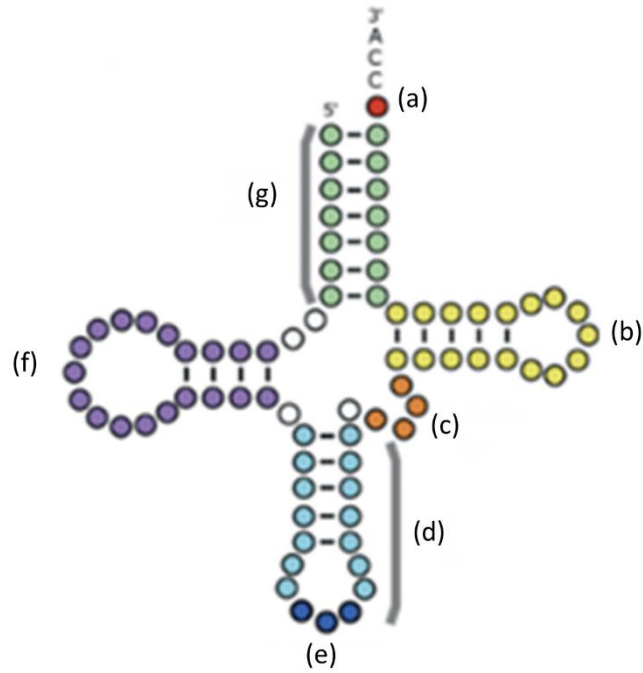


Fig. 3: tRNA secondary cloverleaf structure; (a) discriminator base (73), (b) T ψ C loop, (c) variable arm, (d) anticodon arm, (e) anticodon wobble position, (f) DHU loop, (g) acceptor stem with a 5'-terminal phosphate group (modified from Berg et al., 2019).

Following synthesis, the tRNAs obtain a few enzymatically introduced post-transcriptional modifications to become functional and stable (Paris et al., 2012). Currently, more than 100 unique modifications have been identified (Fig. 4) and, in addition, each modification affects the structure and function in a different way (Schaffer et al., 2019). The most modified are the eukaryotic tRNAs, followed by bacteria, while plastid and parasitic tRNAs have the least number of modifications (Lorenz et al., 2017). Some of these modifications are found in the tRNA core region, such as methylation and pseudouridylation in the D-arm and T-arm, respectively, that stabilize the tertiary structure (Lorenz et al., 2017). However, most modifications are concentrated in the anticodon stem-loop, either directly in the wobble position (34) or close to it (37), that are necessary for translational accuracy (Tuorto & Lyko, 2016).

		Second letter				
		U	C	A	G	
First letter	U	UUU } Phe UUC } UUA } Leu UUG }	UCU } UCC } Ser UCA } UCG }	UAU } Tyr UAC } UAA Stop UAG Stop	UGU } Cys UGC } UGA Stop UGG Trp	U C A G
	C	CUU } CUC } Leu CUA } CUG }	CCU } CCC } Pro CCA } CCG }	CAU } His CAC } CAA } Gln CAG }	CGU } CGC } Arg CGA } CGG }	U C A G
	A	AUU } AUC } Ile AUA } AUG Met	ACU } ACC } Thr ACA } ACG }	AAU } Asn AAC } AAA } Lys AAG }	AGU } Ser AGC } AGA } Arg AGG }	U C A G
	G	GUU } GUC } Val GUA } GUG }	GCU } GCC } Ala GCA } GCG }	GAU } Asp GAC } GAA } Glu GAG }	GGU } GGC } Gly GGA } GGG }	U C A G

Fig. 5: The degeneration of the genetic code (adapted from <https://courses.lumenlearning.com>).

1.5 Queuosine modification of tRNA (Q-tRNAs)

1.5.1 Queuosine

As previously mentioned, most modifications are present in the wobble position of the anticodon loop, which is critical for translational efficiency and accuracy, codon recognition, stress response, cell signaling, metabolism, and bacterial virulence (Vinayak & Pathak, 2010; Yuan et al., 2019). One of these modified nucleotides is queuosine (Q), the modified corresponding base of which is queuine. Queuosine, a hypermodified analogue of guanosine (G), is found in the first wobble position (34) of tRNAs that contain the “G₃₄U₃₅N₃₆” anticodon sequence, where ‘N’ indicates any of the canonical nucleotides (A, C, G or U, respectively). This modification is found in four specific tRNAs – Asn_{GUU}, Asp_{GUC}, His_{GUG} and Tyr_{GUA}. The structure of the Q molecule is defined as 7-(3,4-trans-4,5-cis-dihydroxy-1-cyclopenten-3-yl-aminomethyl)-7-deazaguanosine (Fig. 6) (Vinayak & Pathak, 2010).

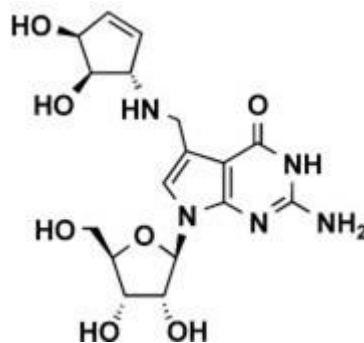


Fig. 6: The structure of queuosine (adapted from Klepper et al., 2007).

Importantly, the presence of Q in the wobble position suggests that it may affect codon usage or frameshifting. Specifically, *in vivo* study in *Xenopus laevis* oocytes showed that Q-tRNAs do not exhibit a preference for either NAU or NAC codons and recognize them with the same affinity, in contrast to unmodified G-tRNAs that prefer NAC codons (Meier et al., 1985). Moreover, *in silico* analysis of codon bias showed a difference between NAU and NAC codons, when the ratio of the codon usage is much lower in onco-developmental than in housekeeping gene transcripts (Morris et al., 1999). Recently, a study on mammalian cells showed that the reduced level of this modification has an effect on the translational speed at Q-decoded and near-cognate codons, causing translation deregulation and induction of the unfolded protein response (Tuorto et al., 2018).

Queuosine is ubiquitously present in nearly all domains of life (eubacteria, eukaryotes and archaea) with a few exceptions (e.g. *Saccharomyces cerevisiae* or *Candida albicans*) (Kessler et al., 2018; Zallot et al., 2014) and the modification is catalyzed by the specific enzyme called tRNA-guanine transglycosylase (TGT).

1.5.2 tRNA-guanine transglycosylase (TGT)

TGT is the enzyme that catalyzes Q modification. Although TGT is involved in the modification reaction of all three domains, the process is significantly different for each of them.

Eubacteria are able to form Q *de novo* in multi-step enzymatic synthesis. This pathway begins with a conversion of guanine to preQ₁ (queuine precursor) utilizing cytosolic GTP. Subsequently, preQ₁ serving as a bacterial TGT (bTGT) substrate is inserted into the corresponding tRNA species, where it is further modified by two enzymes to form fully functional queuine (Biela et al., 2013). Hereafter the Q-tRNA is involved in normal cellular functions until it is destroyed by natural turnover process as a consequence of which Q and/or q are released into the microenvironment (Fergus et al., 2015).

However, for eukaryotes it is necessary to obtain the Q precursor, the free base queuine (q), from dietary sources and/or intestinal microbiota, as they are unable to synthesize it *de novo* due to the absence of required specific enzymes. In contrast to prokaryotes, whose bTGT cannot use the q as a substrate, here is the queuine directly recognized by eukaryotic TGT (eTGT) and irreversibly incorporated in a single enzymatic step in place of guanine into position 34 of tRNAs by a base-exchange reaction (Biela et al., 2013; Fergus et al., 2015). The queuine is salvaged from the environment by DUF2419 protein family found in most

eukaryotes. There are homologues of DUF2419 found in *S. pombe*, *Zea mays*, human and *Sphaerobacter thermophilus*. The enzymatic function of this protein has not yet been elucidated, however, a ribonucleoside hydrolytic activity is expected as it is structurally similar to DNA glycosidases (Zallot et al., 2014). The structure of the eukaryotic Q-tRNA is shown in Fig. 7.

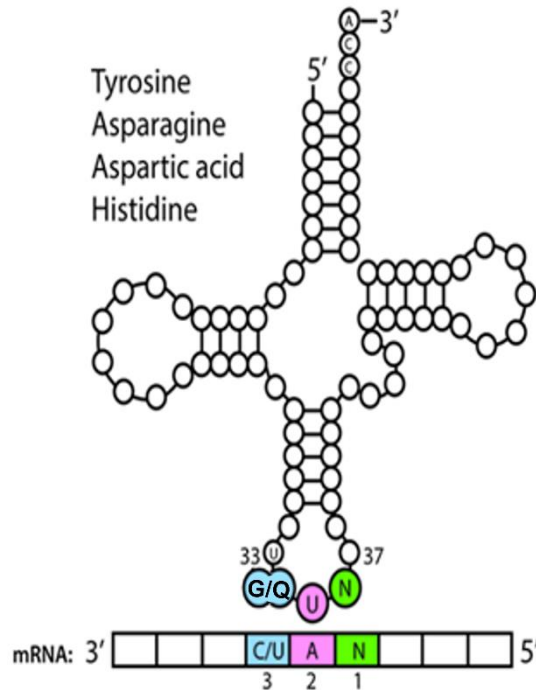


Fig. 7: Queuosine tRNA modification in eukaryotes (modified from Fergus et al., 2015).

Contrary to bTGT, which exists as a homodimer (Romier et al., 1996), eTGT predominantly forms heterodimers composed of the queuine tRNA ribotransferase 1 (QTRT1) and queuine tRNA ribotransferase domain containing 1 (QTRTD1). Although their sequences are significantly different, both of these queuine-insertase subunits are essential for *in vivo* formation of Q-tRNA (Fergus et al., 2015). Furthermore, QTRT1 subunit alone contains conserved residues that are in charge of the catalysis, while QTRTD1 may be involved in the stabilization, as well as it has been implicated as the salvage enzyme generating a queuine from queuosine monophosphate after tRNA turnover (Chen et al., 2010; Vandenberg et al., 2003).

While bTGT is present in eubacteria and eTGT in eukaryotes, in the archaea domain, there is archaeal TGT that inserts archaeosine, a cognate molecule to Q, at position 15 of the D-loop usually to stabilize the canonical L-shape of many tRNAs (Phillips & de Crécy-Lagard, 2011).

1.5.3 Role of Q-tRNAs in physiology

The fact that Q-tRNAs are present in almost all organisms suggests its likely essential role in physiology. There have been several studies in various species with different results. In *Clamydomonas reinhardtii* (Kirtland et al., 1988) and *Caenorhabditis elegans* (Gaur et al., 2007), no developmental or phenotypic effects were observed due to a lack of Q. By contrast, the effect of Q was reported in *Dictyostelium discoideum*, where it affected early developmental processes (Schachner & Kersten, 1984) or lactate metabolism (Schachner et al., 1984), as well as in *Drosophila melanogaster*, where the organism showed a reduced ability to respond on certain stress stimuli (Siard et al., 1991) or increased resistance to the effects of certain heavy metals (Christie et al., 1982). In mammals, the Q-tRNA has been reported to be associated with leukemia (Ishiwata et al., 2001; Singhal et al., 1981), cancer cells formation and tumor growth (Fergus et al., 2015; Katze & Beck, 1980; Randerath et al., 1984), and encephalomyelitis (Varghese et al., 2016). The research on mice has shown that on a Q-deficient diet they were asymptomatic and able to develop, reproduce and survive for up to one year (Reyniers et al., 1981). However, the following study examined that if the non-essential amino acid tyrosine was removed from the Q-free diet, it resulted in neurological issues and all mice died after 18 days. This observation indicates that tyrosine becomes an essential AA in the absence of queuine. Adding either queuine or tyrosine back to the diet returned the mice to the asymptomatic condition (Marks & Farkas, 1997). This phenomenon occurred even though phenylalanine, from which tyrosine can be synthesized by phenylalanine hydroxylase (PAH) enzyme, was included into the diet. In additional studies, it was explained that absence of Q/TGT causes increased oxidation of tetrahydrobiopterin (BH₄), an essential cofactor of PAH, thereby reducing the capacity of tyrosine synthesis (Rakovich et al., 2011). Further investigations to study the exact role of Q in this process are required.

1.6 Codon biased translation

As already mentioned, the genetic code is degenerate, that means that one AA is coded by more than one codon (Crick, 1966), where the codons encoding the same AA are known as ‘synonymous codons’. It has been shown that some of these synonymous codons are preferred over the others during translation. In other words, the synonymous codons are not used with equal frequency. This phenomenon is termed codon usage bias (Behura & Severson, 2013). The presence of codon bias has been reported in all prokaryotic and eukaryotic genomes and each type of genome has its own codon usage strategy. However, closely related organisms can show almost identical biased codon usage (Grantham, 1980; Grantham et al., 1981).

According to another evidence, there has also been suggested an association between the population of tRNAs and codon usage (Ikemura, 1981).

Usually, there are two options by which the preferential use of the synonymous codons is explained. The first of them, the selective model, postulates that there is a co-evolution or co-adapted state between the synonymous codon usage and the tRNA gene content which leads to optimal translation efficiency. Furthermore, different AAs may have different preferred codons, which is explained by the fact that this co-evolution can lead to more than one stable state (Higgs & Ran, 2008). The second model is known as a neutral model in which are biases created in mutational processes (Duret, 2002).

It was long time believed that the major cause of codon usage bias is a selection for efficient and accurate translation; this means, to increase the translation speed and also reduce the translation effort, the organism preferentially uses more rapidly translated codons. These codons are usually those that correspond to the most abundant tRNAs in the cell (Higgs & Ran, 2008). However, the correlation between the codon usage and tRNA abundancy has been demonstrated only in some species (Dong et al., 1996; Ikemura, 1981). This search has failed in several organisms and some following studies showed that this might not be the major factor affecting the codon usage (Duret & Mouchiroud, 1999; Kanaya et al., 2001; Reis, 2004). In fact, there are many other reports to prove that this hypothesis is incorrect because of the role of tRNAs in the stress response, in which the tRNA modification levels change, resulting in alteration in preferred codons so that rare codons are favored. As a result, the translation efficiency is higher for the stress response transcripts (Fig. 8) (Novoa & Ribas de Pouplana, 2012).

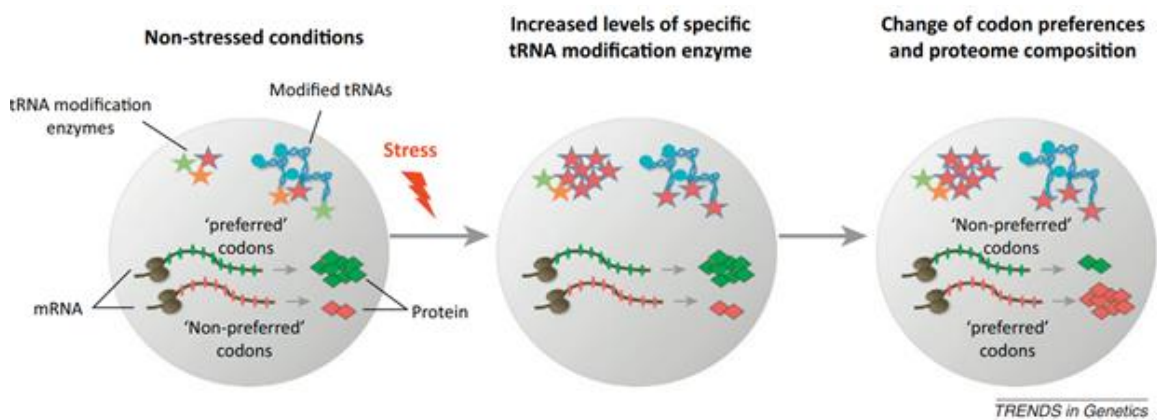


Fig. 8: Modulating of translation during stress response by tRNA modifications through codon usage bias (adapted from Novoa & Ribas de Pouplana, 2012).

It is also suggested that the not-well correlation between codon usage and tRNA composition in bacteria and eukaryotes may be influenced by the presence of two modifications at the wobble position catalyzed either by tRNA-dependent adenosine deaminases (ADATs) or tRNA-dependent uridine methyltransferases (UMs) (Novoa et al., 2012). Notably, in *Saccharomyces cerevisiae* *in vivo* study using genome-wide ribosome profiling method revealed that synonymous codons preferentially used in highly expressed genes have similar translation speed as non-preferred codons. Surprisingly, there was observed the correlation between codon usage and tRNA abundancy. Therefore, it is thought that the codon bias observed in highly expressed genes was created during the process of natural selection to ensure an overall cellular efficiency, rather than translation efficiency, which is provided as a product of stronger selection in highly expressed genes (Qian et al., 2012).

Additionally, patterns of variable codon distribution that may affect ribosomal speed and translation stability are found along genes. It is known that the translation speed varies in different mRNA transcript regions (Arava et al., 2003) Specifically, the reduced speed is at the first 30 – 50 codons, a region called ‘translation ramp’, and then accelerates (Tuller et al., 2010), which confirms the previous *in vivo* ribosome profiling analysis determining densities along mRNAs (Ingolia et al., 2009).

The codon bias and translation speed also play a role in protein folding. Usually, the folding of proteins is co-translational, which is supported by the fact, that the translation of certain protein is paused at specific site by ribosomes (Kim et al., 1991; Yanagitani et al., 2011). The pausing is suggested to be caused by local mRNA structure, which is responsible for the proper protein folding (Cortazzo et al., 2002; Saunders & Deane, 2010). The folding of all regions of a certain protein does not proceed at the same speed, because protein structure is different in the complexity. Hence, the translation speed needs to be adjusted, for which codon usage is used. Two types of regions are distinguished here: the one consisting of ‘slow codons’ and the other of ‘fast codons’. The regions of slow codons are used during the folding of greatly complex protein sequences to ensure sufficient time (Hanson & Collier, 2018).

The codon usage bias has also been found in kinetoplastid protozoans, including trypanosomatids (e.g. *Trypanosoma cruzi*, *Trypanosoma brucei* or *Leishmania major*) (Alvarez et al., 1994; Necşulea & Lobry, 2006; Parsons et al., 1991) and according to the findings, the translational selection appears to be the major control mechanism of the variable protein expression in trypanosomatids. Recently, it has been shown that mRNA and protein

abundance are controlled through codon bias (de Freitas Nascimento et al., 2018; Jeacock et al., 2018).

1.7 Queuosine modification in *Trypanosoma brucei*

A closely related organism of *Leishmania mexicana*, belonging to the same class Kinetoplastida, is *Trypanosoma brucei*, which causes vector-borne disease, ‘African trypanosomiasis’ or sleeping sickness in humans and ‘nagana’ in cattle and horses, transmitted between mammalian hosts by tse-tse fly (Luzak et al., 2021). *Trypanosoma brucei* is a dixenous parasite with procyclic and bloodstream form, meaning that it has to adjust to different environments during its life cycle (Fenn & Matthews, 2007). The most characteristic feature of these species is their circular kinetoplastid DNA, the form of mitochondrial DNA. However, no tRNAs of *T. brucei* are encoded by the kinetoplast (it means, in the mitochondria). Thus, a full set of tRNAs is imported from the cytosol into the organelles (Simpson et al., 1989).

Queuosine modification was also found in *Trypanosoma brucei*. Recently, several works have been published with a great contribution of the members of our own laboratory. One of them showed that Q modification is present in all four previously mentioned specific tRNAs (see section 1.5) in *T. brucei*. In this work was also demonstrated the presence of a retrograde nuclear import pathway which is necessary for the formation of queuosine and for the maturation of tRNA^{Tyr} in *T. brucei* (Kessler et al., 2018).

In another recent publication two paralogs of TGT were identified, TbTGT1 homologous to human QTRT1 and TbTGT2, both of which are essential for Q modification in tRNAs. Moreover, both are located in the nucleus and interact to create a heteromeric complex. In addition, there was confirmed the inability of *T. brucei* to synthesize queuine as well as the dependence of the Q-tRNA modification level on the presence of queuine in the microenvironment. Queuosine has also been found to be significant in codon biased translation. Further observation yielded a result showing the preference of mitochondria to import modified Q-tRNAs from the cytosol rather than unmodified ones. Furthermore, reduced protein synthesis and effects on mitochondrial function were observed when mitochondria were not given enough queuosine. In conclusion, Q modification plays a significant role during mitochondrial translation (Kulkarni et al., 2021).

In the bloodstream form of the parasite, it was observed that both TbTGT1 and TbTGT2 are essential for Q modification, but a significant growth phenotype was demonstrated only in

TbTGT1. In addition, the absence of Q modification delayed the emergence of parasites in the mice's blood that led to prolonged mice survival. Besides this, it was found that parasites isolated from mice showed higher levels of Q modification than the cultured cell line (Kulkarni, 2021).

Different levels of Q modification in procyclic and bloodstream stage were supported in the following publication. The indirect correlation was found between the amount of certain AAs (namely tyrosine, cysteine, and glutamate) and the Q-tRNA content. Moreover, changes in the AAs concentration caused alterations in Q modification levels. Additionally, tyrosine deficiency resulted in the accumulation of the nuclear tRNA^{Tyr} and if the concentration of tyrosine was changed, the Q content also changed. Last but not least, another pivotal experiment confirmed the importance of queuosine in the nutrition driven codon biased translation (Dixit et al., 2021).

1.8 Rationale of the project

Trypanosomatids are the causative agents of several serious diseases transmitted by different insect vectors. These protists are characterized by polycistronic transcription of their protein-coding genes (LeBowitz et al., 1993; Ullu et al., 1993). Moreover, in trypanosomatids, no RNA polymerase II promoters have been identified (McDonagh, 2000) and therefore considerable emphasis is placed on post-transcriptional mechanisms or events (Shapira et al., 2001). As a result, trypanosomatids provide a unique chance to investigate post-transcriptional control mechanisms of the gene expression.

The experimental model chosen here, *Leishmania mexicana*, causing a leishmaniasis disease, is a well-established organism with whole sequenced genome (Rogers et al., 2011) implemented in the source TriTrypDB (Aslett et al., 2010). Easy cultivation, short time of cell division and the possibility of using several tools of genetics and molecular biology are other advantages of *Leishmania*.

Considering the results obtained in the *T. brucei* experiments, which were described in the previous chapter, we hypothesized that in closely related organism such as *Leishmania*, the queuosine modification might also play a significant role. Based on the previous results from our laboratory, we know that, in *Leishmania in vitro* study also have been found two paralogs of TGT, LmxTGT1 and LmxTGT2 with no significant growth phenotype in LmxTGT2 KO strain. However, a reduced ability to infect macrophages and multiply inside them has been demonstrated in LmxTGT2 KO strain, as well as a more difficult transition during the

differentiation from the metacyclic to the amastigote life stage. *In vivo* experiments showed reduced size in lesions in mice ears that were injected with LmxTGT2 KO parasites. The same study also examined a dependence of the lesion progression on the numbers of the parasites at the infection site (Boudová, 2018).

Therefore, we decided to build on these findings, include a previously created add-back cell line in this project, and try to standardize several methods such as polysome or ribosome profiling in *Leishmania mexicana* in order to provide a greater understanding of the Q modification effects on another experimental system, which has not yet been fully explored. Moreover, unlike *T. brucei*, in *Leishmania mexicana* it is possible to perform a complete life cycle *in vitro* and therefore we decided to study how Q affects the development. In addition, during a previous experiment in our lab, there was a technical issue in the ribosome profiling of bloodstream stage in *T. brucei* because it is necessary to isolate the parasites, which takes from 30 minutes to one hour and this delay may cause artifacts in the library. It was also complicated to isolate the bloodstream form parasites at early stages of the infection when the phenotype of Q can be observed (Kulkarni, 2021). Therefore, it is easier to study the role of Q in infection in *Leishmania*. Hence, we decided to expand our experimental system.

2 Aims of the thesis

1. To standardize the polysome profiling and ribosome profiling method for *L. mexicana*.
2. To elucidate the role of queuosine in translation using ribosome profiling.
3. To study the role of queuosine in translation using proteomics.
4. To study the role of queuosine in *L. mexicana* cell cycle.

3 Materials and methods

3.1 Cell culture

Three *Leishmania mexicana* cell lines were employed in the experiments: wild type (WT) cell line, knock-out (TGT KO) cell line, and add back (AB) cell line. RNDr. Mgr. Michala Boudová kindly provided the TGT KO and AB cell lines, which were generated as described previously (Boudová, 2018). The cell lines were cultivated in M199 medium (Sigma-Aldrich, Cat. No. M0393-10X1L) with 2 µg/ml hemin (Sigma-Aldrich, Cat. No. 51280-5G), 5 µg/ml bioperin (Sigma-Aldrich, Cat. No. B2517-50MG), 100 mg/ml penicillin-streptomycin (Sigma-Aldrich, Cat. No. P4333-100ML), 25 mM HEPES (Glentham Life Sciences, Cat. No. GM5581), 10% sterile heat-inactivated fetal bovine serum (FBS) (Sigma-Aldrich, Cat. No. F7524-500ML) and 100 µg/ml hygromycin (Hyg) (Invivogen, Cat. No. ant-hg-1). The medium was adjusted to pH 7.4. The medium used for maintenance of the TGT KO cell line was additionally supplemented with 50 µg/ml puromycin (Puro) (Invivogen, Cat. No. ant-pr-1) and 100 µg/ml nourseothricin (Ntc) (Jena Bioscience, Cat. No. AB-102L), an additional 5 µg/ml phleomycin (Phleo) (Invivogen, Cat. No. ant-ph-1) was added to the AB medium. The cultures were maintained at 25°C.

For cell counting, 50 µl of cell culture was fixed with 10% formalin solution (see Annex 1a), and counted using Neubauer haemocytometer (Sigma-Aldrich, Cat. No. BR717805-1EA). In order to keep the cells in logarithmic phase of growth, they were diluted to 2×10^5 cells/ml once per 72 hours or according to specifications in the protocols.

3.2 Isolation of RNA

Isolation of RNA was performed as described previously (Chomczynski & Sacchi, 2006) with modifications. In brief, cells were harvested by centrifugation (1 300 g, 10 min, room temperature), washed with PBS (see Annex 1b) and resuspended in 500 µl Solution D (see Annex 1c). 50 µl 2M NaOAc (pH 4.0) was then added, and the sample was extracted with 500 µl H₂O saturated phenol (PanReac AppliChem, Cat. No. A1624,0500) and 150 µl chloroform/IAA (24:1) (Lach:ner, Cat. No. 20034-AT1). This was followed by vortex for 1 min, placing on ice for 10 min and centrifugation (12 000 rpm, 15 min, 4°C). The aqueous phase was transferred to the new Eppendorf tube. In order to precipitate the sample, equal amount of isopropanol (Lach:ner, Cat. No. 20037-AT0-M1000-1) and 1 µl glycogen (Sigma-Aldrich, Cat. No. G1767-1VL) were added, the sample was then stored at -20°C for 30 min/overnight, centrifuged (15 000 rpm, 30 min, 4°C) and washed with 70% ethanol

(Lach:ner, Cat. No. 20025-A96-M1000-1). RNA pellet was dissolved in 200 µl MilliQ® water and extracted with 0,5V phenol (pH 8.0) and 0,5V chloroform/IAA. The aqueous phase was precipitated again with 3V ethanol, 0,1V 3M NaOAc, 1 µl glycogen, washed with 70% ethanol and dissolved in 30 µl MilliQ® water. Concentration and purity of RNA were measured using the NanoDrop™ 1000 Spectrophotometer (Thermo Fisher Scientific).

3.3 Boronate affinity electrophoresis and northern blotting

Boronate affinity electrophoresis was carried out as described previously (Igloi & Kössel, 1985) with modifications. Briefly, 5 µg of total RNA was deacetylated by adding 100 mM Tris-HCl (pH 9.0) and incubated at 37°C for 30 min. The sample was precipitated with ethanol, washed with 70% ethanol, and resuspended in 6 µl urea loading dye (see Annex 2a). One of the samples was employed as periodate-oxidized technical control. This RNA pellet was resuspended in MilliQ® water, incubated in 50 mM NaOAc (pH 5.2) and 2,5 mM NaIO₄ for 2 hours at 37°C in the dark, 2mM glucose was then added to inhibit the reaction and the sample was incubated 30 min at 37°C in the dark, followed by purification by Sephadex™ G25 (GE Healthcare, Cat. No. 17-0572-02) column, ethanol precipitation and resuspension in urea loading dye. The samples were denatured at 70°C for 10 min and loaded on the gel.

In the gel solution (1x TAE (see Annex 2b), 8M urea (MP, Cat. No. 191450), 8% acrylamide) was dissolved 3-(Acrylamido)phenylboronic acid (APB) (Sigma-Aldrich, Cat.No. 771465- 1G) at room temperature for 30 min. Subsequently, 60 µl 10% APS and 10 µl TEMED (Bio-Rad, Cat. No. 161-0800) were added for casting. Electrophoresis was performed at 4°C, 75V for 5 hours. The gel was then stained with ethidium bromide (EtBr) (CarlRoth, Cat. No. 2218.1) and visualized by ChemiDoc™ MP (Bio-Rad).

The RNA was transferred from the gel to ZETA probe membrane (Bio-Rad) in 0,5x TAE at 150 mA for 90 min, once transferred, the membrane was dried and UV cross-linked (Stratagene, Stratalinker® UV Crosslinker).

3.4 Oligonucleotide hybridization

Following the northern blotting, the membrane was pre-hybridized at 48°C for 0,5 – 1 hour in hybridization solution (see Annex 2c, 2d). The sequences of oligonucleotides used for hybridization are listed in Annex 4a. For radioactive labelling, these oligonucleotides were mixed with T4 Polynucleotide kinase (PNK) (New England Biolabs, Cat. No. M020L) and γ -³²P ATP (Hartmann Analytic, Cat. No. FP-401, 9,25 MBq) and incubated 1 hour at 37°C. Subsequently, the probes were purified by Sephadex™ G25 column (3 200 RPM, 2 min, room

temperature), denatured at 100°C for 5 min, and chilled on ice for 2 min. The probe was then transferred into the hybridization solution and the membrane was hybridized at 48°C overnight. Subsequently, the membrane was washed at 48°C, with wash buffer 1, followed by wash buffer 2 (see Annex 2e, 2f) for 20 min each, exposed to Phosphoimager screen (GE Healthcare) overnight and developed using Typhoon scanner (Molecular Dynamics). The membrane was stripped by boiling in stripping solution (see Annex 2g) at 80°C for 2x 20 min and stored in the stripping solution for next hybridization.

3.5 Pulse labelling of proteins

Pulse labelling to measure protein synthesis was performed as described previously with modifications (DeCaprio & Kohl, 2018). Briefly, 2×10^7 cells were harvested by centrifugation (2 000 g, 10 min, room temperature), resuspended in 500 µl methionine-free medium (M199 medium) and incubated at 25°C 15 min. The [³⁵S]Met-label (10 µCi at about 800 Ci/mmol) (Hartmann Analytic, Cat. No. SCIS-103, 185 MBq) was then added, samples were incubated at 25°C for 30 min and proceeded for analysis of protein synthesis or protein aggregates.

3.6 Analysis of protein synthesis

In order to examine the total protein synthesis pattern, the cells were pelleted by centrifugation (1 300 g, 5 min, room temperature), washed with PBS 2 times and resuspended in 50 µl 2x Laemmli sample buffer. The samples were heated at 100°C and separated by SDS-PAGE (4-20%, Bio-Rad). The gel was then stained with Coomassie (approx. 2 h), de-stained (approx. 4 h) and dried using the Gel Dryer (Bio-Rad). The dry gel was exposed to the Phosphoimager screen (GE Healthcare) overnight and developed using Typhoon scanner (Molecular Dynamics).

3.7 Analysis of protein aggregates

Analysis of protein aggregates was performed as described elsewhere (Koplin et al., 2010; Nedialkova & Leidel, 2015) with modifications. In brief, the cells were washed with PBS, resuspended in lysis buffer (see Annex 3a), incubated at room temperature for 20 min and chilled on ice. The chilled samples were then sonicated using Ultrasonic Homogenizer (6 times at level 4, 50% amplitude) and spun (200 g, 20 min, 4°C). The supernatants were transferred to fresh Eppendorf tubes and the aggregated proteins were pelleted by centrifugation (16 000 g, 20 min, 4°C). The protein aggregates were resuspended twice in 500 µl wash buffer (see Annex 3b) and sonicated as before. The samples were centrifuged (16 000 g, 20 min, 4°C), washed with NP-40-deficient wash buffer and sonicated (4 times at level 2, 65% amplitude).

These samples were then divided into 2 tubes, one of them was sent for proteomics and the second was separated by the SDS-PAGE, Coomassie stained and developed as described above.

3.8 Polysome isolation

3.8.1 Cell lysis

Previously described (Tinti et al., 2021) protocol was standardized for *L. mexicana*. In brief, 1×10^9 cells growing at the density of 5×10^6 cells/ml were harvested by centrifugation (1 300 g, 5 min, room temperature) and resuspended in 500 μ l PDC buffer (see Annex 1d). Cells were lysed by adding 20% IGEPAL (final concentration 0,2% v/v) (Sigma-Aldrich, Cat. No. I3021-50ML) and 5 μ l TURBO DNaseI and incubated on ice for 10 min. The lysate was then passed through 24G needle 15 times and centrifuged (15 000 g, 10 min, 4°C). The OD₂₆₀ of cleared lysates was determined using NanoDrop™ 1000 Spectrophotometer (Thermo Fisher Scientific).

3.8.2 Polysome recovery

The polysome buffer with 100 mg/ml cycloheximide (CHX) (Sigma-Aldrich, Cat. No. C7698-1G) was used to prepare 10% and 50% sucrose (PanReac AppliChem, Cat. No. A2211,1000) solutions in order to make the continuous sucrose gradient at 10-50% concentrations. The gradients were performed using Gradient Station (Biocomp). The cleared lysates were then loaded on the top of the sucrose, the tubes were balanced up to 2 digits past the decimal using 10% sucrose and centrifuged (36 000 rpm, 2 h, 4°C, vacuum) using Optima XPN-90 Ultracentrifuge (Beckman Coulter™). The polysome profile was obtained using Gradient Station, fractions were collected using Fraction Collector FC 203B (Gilson) and proceeded for RNA isolation.

Several different conditions were used to standardize this method for *L. mexicana*. All standardization methods were performed with 10 OD samples. The value for the samples used in the final method had been increased to 40 OD. Firstly, in the original protocol 1mM DTT was added to the PDC buffer. Removal of this reagent did not cause any differences, so we continued without DTT. Secondly, it was tested the increase of the total number of cells to 5×10^7 . The addition of other detergents, NP₄₀ (MP Biomedicals, Cat. No. 0219859690) and also 20% Triton X-100 (Sigma-Aldrich, Cat. No. 9036-19-5), instead of IGEPAL, was chosen as another standardization condition. It has also been tested what effect on the final profile would have a passage through 24G needle only 5 times, instead of 15 times. In addition, three

different concentrations of IGEPAL – 10%, 20%, and 30% - were tested. The next step was adding of 100 mg/ml CHX and incubation at 25°C for 5 minutes before harvesting. Lastly, the effect of adjusting the OD in all samples to exactly the same value was observed.

3.9 Ribosome profiling

3.9.1 Cell lysis

The cell lysis for ribosome profiling was performed as described previously (Brar & Weissman, 2015) with modifications mentioned in paragraph 3.8.1.

3.9.2 RNase digestion and ribosome recovery

The RNase digestion was performed by adding RNase I (1 600 units), the samples were incubated on ice for 50 min and the reaction was inhibited by adding SUPERase*In (100 units). The ribosome recovery protocol is described in paragraph 3.8.2.

As with the polysome profiling method, this method also had to be standardized for *L. mexicana*, which was done through the following conditions. First, the technique was checked by comparing the sample treated with RNase I with untreated sample and control sample (*T. brucei*). Next, the 20 OD sample was divided into two 10 OD samples to get maximum digestion in each sample. Another condition was to test the effect of three different incubation times on ice – 40, 50, and 60 minutes.

3.9.3 RNA isolation from sucrose fractions

The isolation of RNA from sucrose fractions was done using the phenol:chloroform extraction protocol with modifications. Briefly, 80S sucrose gradient fractions were added to the pre-warmed acid phenol (65°C, with the ratio of phenol:sucrose fraction 1:1) and vortexed for 20 sec. The samples were then incubated at 65°C for 5 min with vortexing every minute for 10 sec and chilled on ice for 3 min. Subsequently, 100 µl of chloroform was added, the samples were vortexed for 10 sec and spun (10 000 g, 5 min, room temperature). The aqueous phase was then transferred to the clean tube, vortexed 20 sec with 1V of acid phenol and 100 µl of chloroform and spun (10 000 g, 5 min, room temperature). The extraction was performed again with using 800 µl chloroform. The aqueous phase was precipitated with 12 µl glycogen, 80 µl 3M NaOAc and 100% ethanol up to 2 ml. Following the precipitation, 20 µg of RNA was mixed with 20 µl MilliQ®.

3.9.4 Footprint size selection

The 15%PAA/1xNNB/8M urea gel (see Annex 1e, 5a) was pre-run at 400V for 20 min. In the meantime, 20 μ l of RNA Gel Loading Buffer (see Annex 1f) without dyes was added to the RNA. Marker control oligo samples were prepared as follows:

Tab. I: Marker control oligo

Components
20 μ M RNA con 26 nt
20 μ M RNA con 34 nt
20 μ l 2x RNA Gel Loading Buffer with dye

The sequences of the markers are listed in Annex 4b.

All samples were denatured at 80°C for 5 min. Subsequently, each RNA sample was loaded onto the urea gel in two wells, with the control oligo sample on either side, and run 3 hours at 400V. The gel was then stained for 3 min with SYBR Gold (1:10 000 in 1x NNB), visualized using blue-light transilluminator and for each sample 26 nt – 34 nt region was excised. The excised gel slices were placed in a clean non-stick tube and crushed with a plastic disposable pestle. 400 μ l of Gel Elution Buffer (see Annex 1g) was added and the RNA was eluted overnight on the wheel at 4°C.

The gel was spun through the SpinX column (5 000 g, 4 min, room temperature). Flowthrough was collected to a new tube and ethanol-precipitated (12 μ l glycogen, 40 μ l 3M NaOAc, 900 μ l 100% EtOH). Following the precipitation, the pellet was briefly air-dried and resuspended in 40 μ l of MilliQ®.

3.9.5 3' dephosphorylation

The RNA was denatured for 2 min at 80°C and mixed with dephosphorylation reaction (see Tab. II). 1 μ l of 20 μ M 26 nt RNA con was added into 40 μ l of MilliQ® serving as control reaction. The samples were incubated for 1 hour at 37°C and mixed with 20 μ l 3M NaOAc (pH 5.2), 12 μ l glycogen and 118 μ l MilliQ®. The RNA was extracted with acid phenol and chloroform and ethanol-precipitated. The pellet was resuspended in 10 μ l MilliQ®.

Tab. II: Dephosphorylation reaction components.

Component	Volume (µl)
RNA sample	40
10x T4 PNK buffer	5
T4 PNK (NEB)	1
SUPERase*In	1
MilliQ®	3

3.9.6 3' adaptor ligation

5 µl of the dephosphorylated RNA was mixed with 1,5 µl randomized Cloning Linker (0,5 µg/µl; IDT, 5rApp/CTGTAGGCACCATCAAT/3ddC) and the components listed in Tab. III were added. The reaction was incubated for 4 hours at 22°C. Following the incubation, 5 µl glycogen, 20 µl 3M NaOAc (pH 5.2) and 180 µl MilliQ® were added, the samples were extracted and ethanol-precipitated. The pellet was resuspended in 11 µl MilliQ®.

Tab. III: Ligation reaction components.

Component	Volume (µl)
50% PEG 8000	10
10x T4 RNA Ligase buffer	2
T4 RNA Ligase 2 (truncated)	1
SUPERase*In	0,5

3.9.7 Reverse transcription (RT)

Following the ligation reaction, 11 µl of the adapter-ligated RNA was mixed with 1 µl of 10 µM RT oligo (see Annex 4c for the sequence) and the samples were denatured for 5 min at 75°C. The reverse transcription reaction (see Tab. IV) was then added, and the samples were incubated for 40 min at 55°C. In order to hydrolyze the RNA, 2,2 µl 1M NaOH was added to the sample and incubated for 12 min at 98°C. Subsequently, the RNA Gel Loading Buffer without dyes was added to each tube, the marker (1 µl 10 µM RT oligo, 40 µl RNA Gel Loading Buffer with dye) was prepared and all samples were denatured for 5 min at 95°C.

10%PAA/1xNNB/8M urea gel (see Annex 5b) was pre-run at 300V for 20 min, the samples were loaded, and the gel was run at 300V for 2,5 hours. The gel was then stained with SYBR Gold (1:10 000 in 1xNNB), visualized using blue-light transilluminator and the region

corresponding to extended RT oligo was excised. The excised gel slices were placed in a clean non-stick tube, crushed, mixed with 360 μ l MilliQ® and the cDNA was eluted for 20 min at 70°C with vortexing every 10 sec.

The gel was spun through the SpinX column (5 000 g, 4 min, room temperature), collected to a new tube and ethanol-precipitated (12 μ l glycogen, 40 μ l 3M NaOAc, 900 μ l 100% EtOH). Following the precipitation, the cDNA pellet was briefly air-dried and resuspended in 11 μ l of MilliQ®.

Tab. IV: Reverse transcription reaction components.

Component	Volume (μl)
5x FS buffer	4
10 mM dNTPs	1
0,1 M DTT	1
Superscript III	1
SUPERase*In	1

3.10 Flow cytometry

3.10.1 PI staining

The propidium iodide staining for cell cycle analysis was performed as previously described (Riccardi & Nicoletti, 2006). Briefly, 5×10^6 cells were harvested by centrifugation (1300 g, 3 min, room temperature), and resuspended in 300 μ l PBS. The samples were then fixed with 700 μ l methanol and left overnight at 4°C. Following fixation samples were centrifuged (1300 g, 3 min, room temperature), washed with ice cold PBS containing 0,2% Triton X100 and resuspended in PI solution (see Tab. Annex 1h), with one sample left without PI to serve as unstained control. The samples were incubated at 37°C for 45 min and analyzed by BD FACS Canto™ II.

3.10.2 TMRE staining

The analysis of the TMRE membrane potential was performed as described previously (Crowley et al., 2016). Briefly, 5×10^6 cells were harvested by centrifugation (1 300 g, 10 min, room temperature) and the pellet was resuspended in the TMRE media (1 ml M199 media, 60 nM TMRE). One WT sample without TMRE was employed as unstained control. Adding 20 μ M FCCP to one TMRE WT sample served as FCCP control. The samples were incubated at 25°C 30 min with the caps open and harvested by centrifugation (1 300 g, 10 min, room

temperature). The cell pellet was resuspended in 1 ml filtered 1x PBS (pH 7.4). 1ml of 1x PBS was also added in FACS tube, the samples were transferred into the tubes and analyzed by BD FACS Canto™ II.

4 Results

4.1 Evaluation of the presence of Q in Lmx tRNA^{Asp, His, Tyr}

To determine the queuosine content in WT, LmxTGT2 KO and LmxTGT2 AB cell lines, total RNA isolated from each cell line was resolved using boronate affinity electrophoresis followed by ethidium bromide gel staining which showed RNAs divided according to length (Fig. 9). Subsequently, the RNA was transferred to ZETA probe membrane and hybridized with tRNA species-specific ³²P-labeled probes (Fig. 10). Q-free tRNA^{Ile} was employed as negative control, periodate-oxidized RNA (OX) was served as negative control of the technique. Q modification was detected in the WT cell line, in all three tRNAs tested, whereas the KO cell line showed a complete absence of Q. The AB cell line rescued the KO phenotype by restoring the modification.

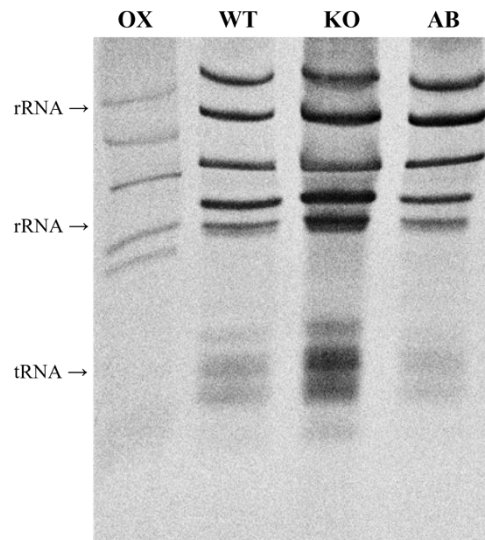


Fig. 9: Ethidium bromide gel staining of total RNA resolved on 8% polyacrylamide-urea gel.

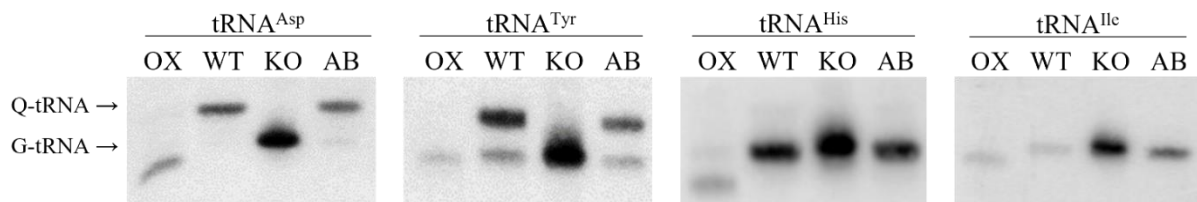


Fig. 10: Northern blotting and hybridization with tRNA species-specific ³²P-labeled probes showed complete Q-depletion in KO cell line and rescue phenotype in AB cell line, in corresponding tRNA. tRNA^{Ile} served as a negative control, OX served as a negative control of the technique.

4.2 Q modification does not affect the growth of *L. mexicana* in axenic culture

The number of cells/ml of WT, LmxTGT2 KO and LmxTGT2 AB cell lines was counted for eight days at the same time with daily dilution to initial seeding density. The growth curve

of each cell line represents an average value of three repeats. The resulting graph showed that there is no significant difference in growth rate between the three cell lines (Fig. 11).

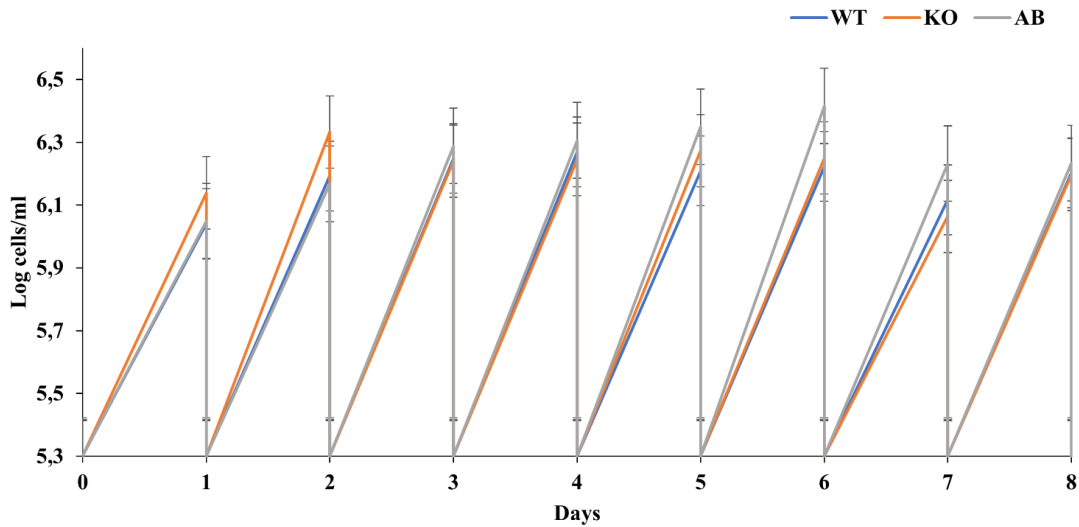


Fig. 11: Growth curves of WT, LmxTGT2 KO and LmxTGT2 AB cell lines monitored for eight days with everyday dilution to 2×10^5 cells/ml. Error bars represent the standard deviation of three independent replicates.

4.3 Q modification does not affect the cell cycle of *L. mexicana*

In order to test the impact of TGT2 KO on the cell cycle, we fixed the cells with methanol, stained with propidium iodide at 37°C for 45 min and analyzed by BD FACS Canto™ II. In the first experiment, the medium was supplemented with antibiotics used for TGT2 KO and AB cell lines. As a result, the graphs show a slightly different phenotype in Q-deficient TGT2 KO cell line as well as in AB cell line compared to WT cell line, especially in S and G2/M phases (Fig. 12). The cells appear as if arrested or slowed down in the G1 phase.

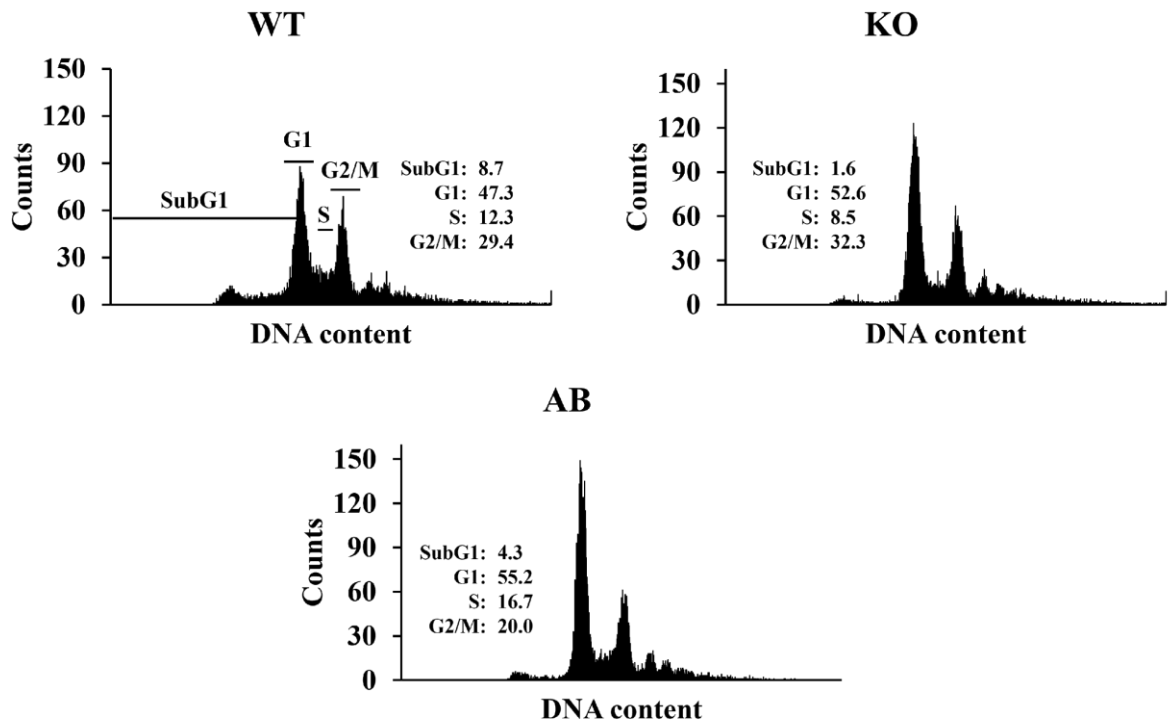


Fig. 12: PI staining for cell cycle analysis. The media supplemented with all antibiotics used for TGT2 KO and AB cell lines. Cell count is plotted on the y-axes. Three biological repeats were performed, and representative histograms are shown. Percent of cells in SubG1, G1, S and G2/M are shown.

The results obtained from the previous experiment led us to hypothesize if the values are not influenced by the supplementary antibiotics in TGT2 KO and AB media and therefore another experiment was performed in which the medium contained only hygromycin for all three cell lines. The resulting graphs showed only a slight difference in the KO cell line as compared to WT and AB (Fig. 13). This slight phenotype is clearly not enough to affect the overall growth of the culture as seen in the previous result (Fig. 11). Moreover, it shows the importance of including of AB cell line to this project (Fig. 13). This point is discussed in more detail in section 5.

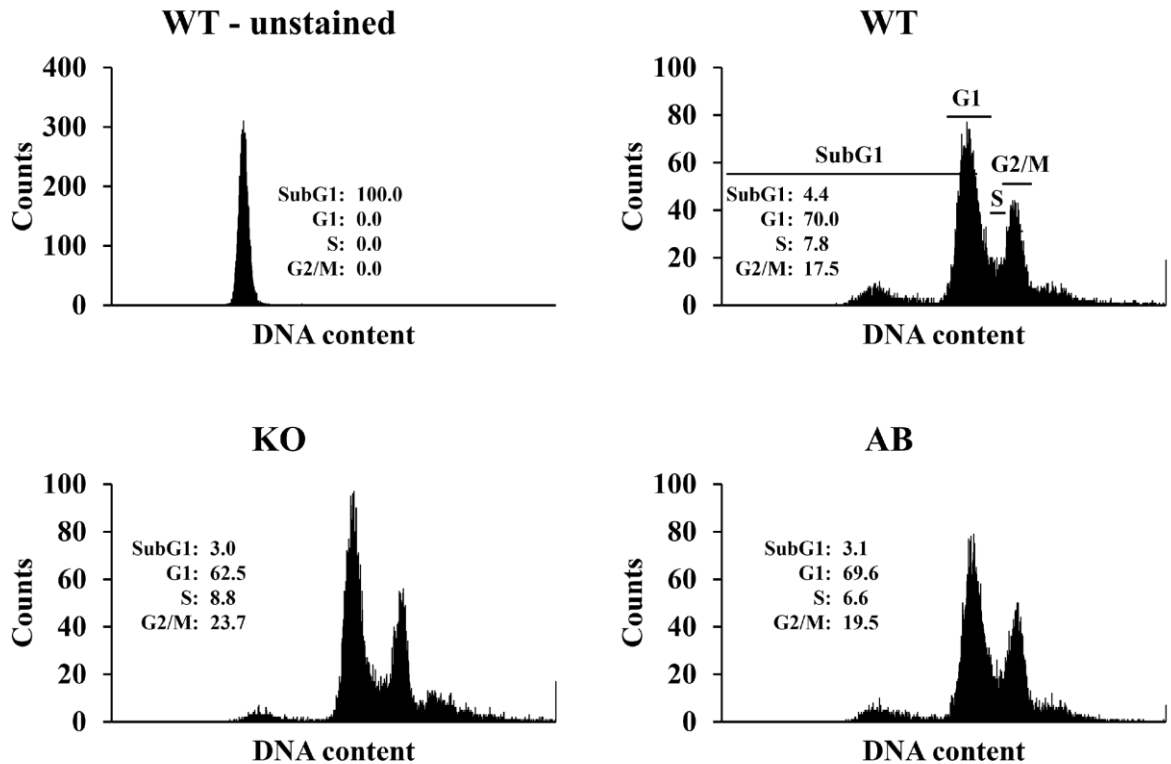


Fig. 13: PI staining for cell cycle analysis. The media supplemented with hygromycin. Cell count is plotted on the y-axes. Three biological repeats were performed, and representative histograms are shown. Percent of cells in SubG1, G1, S and G2/M are shown.

4.4 Q modification does not affect the mitochondrial membrane potential of *L. mexicana* procyclic promastigotes

Although the ablation of TGT2 KO did not significantly affect cell cycle, we tested if the absence of Q could have an effect on mitochondrial membrane potential (MMT). To analyze the MMT, the cells were harvested, stained with positively charged dye, tetramethylrhodamine ethyl ester (TMRE), incubated, centrifugated and resuspended in 1x PBS. The analysis was performed by BD FACS CantoTM II. As positive control of the technique, *T. brucei* procyclic form and FCCP was used. There was no obvious effect on the membrane potential; however, these results are preliminary, as only one biological repeat was performed (Fig. 14).

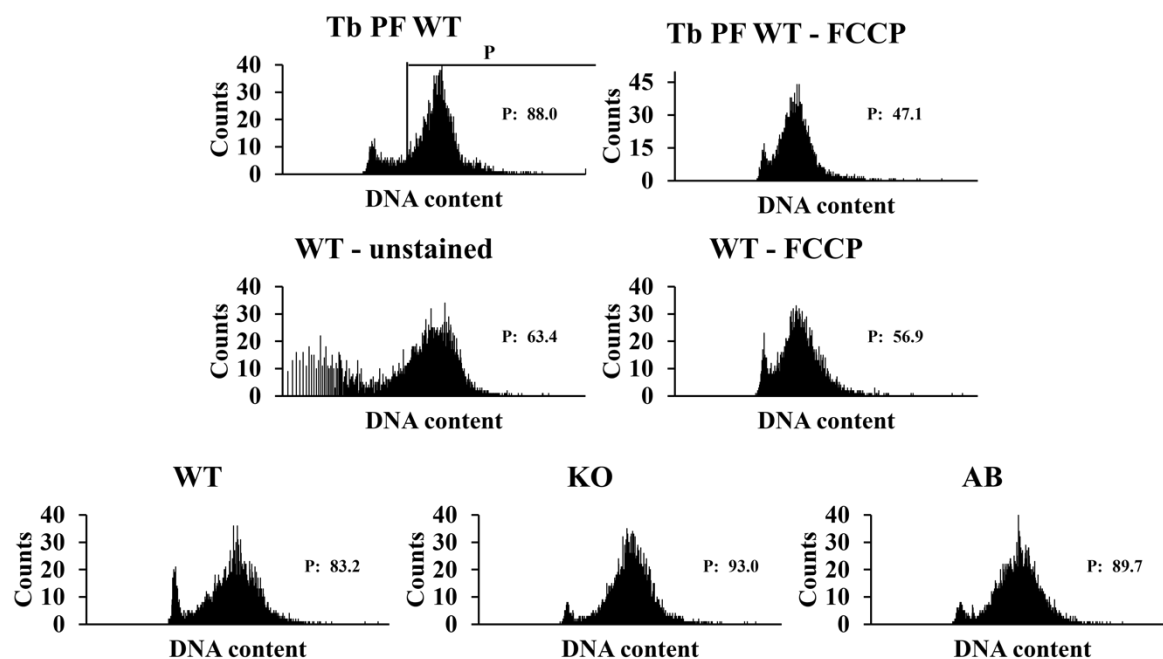


Fig. 14: TMRE staining for membrane potential analysis. *T. brucei* procyclic form used as positive control for the technique (Tb WT). FCCP used as positive control for mitochondrial membrane depolarization. Cell count is plotted on the y-axes. One biological repeat was performed. Percent of cells in P are shown.

4.5 Polysome analysis

4.5.1 Standardization

To standardize the polysome analysis protocol for *L. mexicana*, the first step was to standardize cell lysis conditions for optimum polysome yield. First, we investigated the effect of passage through needle only 5 times as well as two different concentrations of CHX (100 $\mu\text{g/ml}$ and 200 $\mu\text{g/ml}$). Simultaneously, we lysed the cells by using two different detergents – 20% IGEPAL and 10% NP₄₀. As positive control of the technique, lysate of *T. brucei* procyclic form was used (Fig. 15A). We found out that 5 times passage is not enough, the polysomes are not as clearly separated as when passaged 15 times (Fig. 15B, 15E). The resulting graph also shows that 100 $\mu\text{g/ml}$ CHX is a sufficient concentration to obtain a good polysome profile (Fig. 15B, 15C). NP₄₀ detergent was shown to degrade the polysomes (Fig. 15D) and therefore, it is better to use IGEPAL. In conclusion, we decided to passage 15 times and use 100 $\mu\text{g/ml}$ CHX and IGEPAL in further experiments. When we tried to increase the cell density for the experiment to 5×10^7 cells/ml, the resulting polysome profile showed a loss of heavy polysomes, indicating the importance of keeping the cells in early log phase (Fig. 15F). The cell density of 5×10^6 cells/ml was thus found to be optimum in terms of both yield and quality of polysomes (15E).

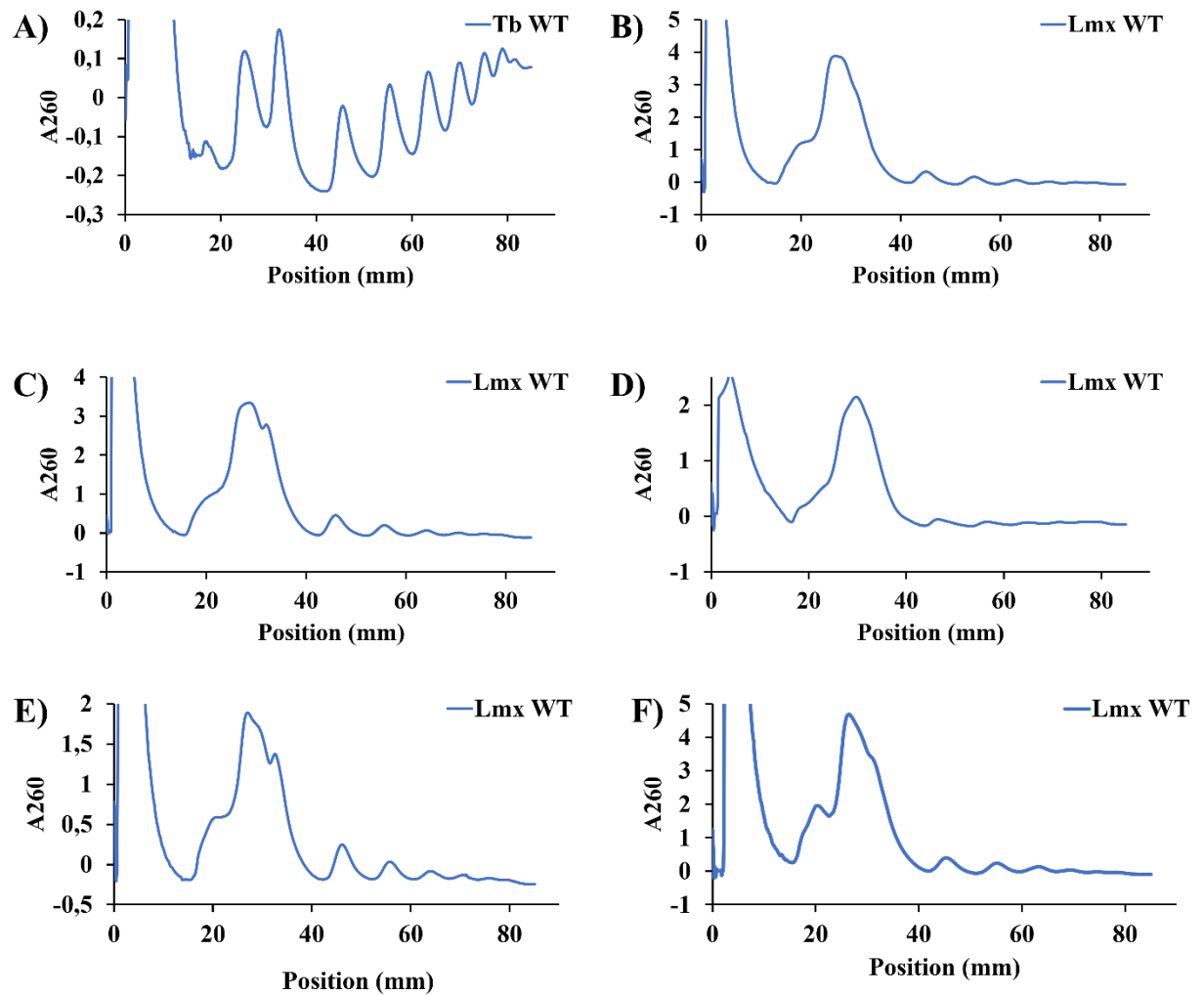


Fig. 15: Polysome analysis. A) *T. brucei* procyclic form lysates used as positive control for the technique (Tb WT); B) Lmx WT, 1x CHX, 5x pass, 20% IGEPAL, no DTT; C) Lmx WT, 2x CHX, 5x pass, 20% IGEPAL, no DTT; D) Lmx WT, 1x CHX, 5x pass, 10% NP₄₀, no DTT; E) Lmx WT, 1x CHX, 15x pass, 20% IGEPAL, no DTT, 5x10⁶/ml; F) Lmx WT, 1x CHX, 15x pass, 20% IGEPAL, no DTT, 5x10⁷/ml.

In another condition for standardization, we used three different concentrations of IGEPAL, 10% (Fig. 16A), 20% (Fig. 16B), and 30% (Fig. 16C). The best heavy polysome distribution was obtained using 20% IGEPAL.

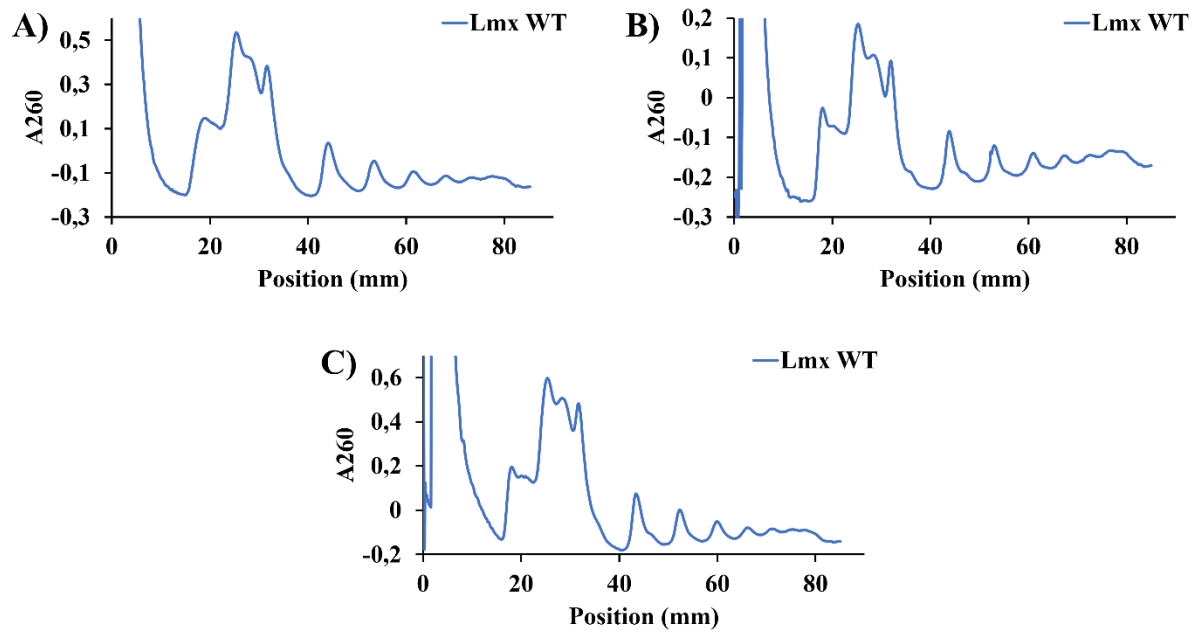


Fig. 16: Polysome analysis. A) Lmx WT, 1x CHX, 15x pass, 10% IGE PAL; B) Lmx WT, 1x CHX, 15x pass, 20% IGE PAL; C) Lmx WT, 1x CHX, 15x pass, 30% IGE PAL.

In the last experiment, the effect of another detergent - 20% TritonX-100 - on the resulting polysome profile was tested and found to be not significantly different from that of IGE PAL (Fig. 17).

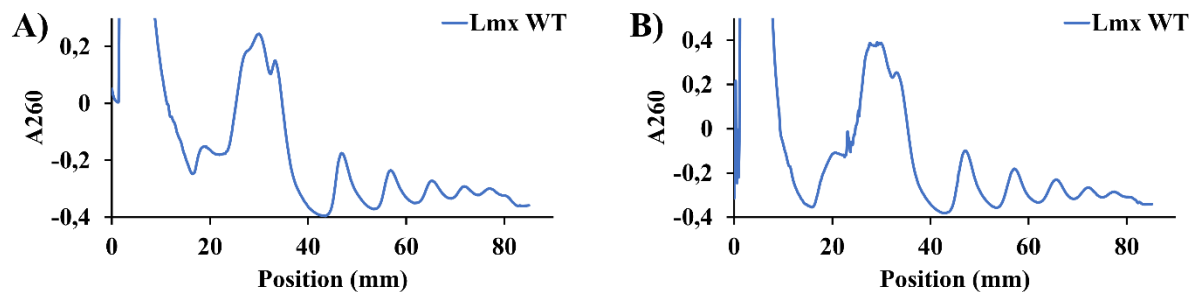


Fig. 17: Polysome analysis. A) Lmx WT, 1x CHX, 15x pass, 20% IGE PAL; B) Lmx WT, 1x CHX, 15x pass, 20% TritonX-100.

4.5.2 Standardized polysome profile for *L. mexicana*

Finally, the standardized conditions for the best polysome profile are as follows: the translation elongation was inhibited by incubation with 100 $\mu\text{g/ml}$ CHX at 25°C for 5 min, 5×10^6 cells/ml were harvested, resuspended in PDC buffer without DTT, lysed by 0,2% IGE PAL and TURBO DNaseI, passed through 24G needle 15 times and centrifuged. The resultant lysates were then loaded on a continuous 10 – 50% sucrose gradient, ultracentrifuged at 36 000 rpm for 2 hours, fractionated and absorbance at 260 nm was recorded. In the resulting graph we see the overall degree of translation in cells. The polysome profile showed a peak

containing the untranslated mRNA and other free RNAs, then the small ribosomal subunit, large ribosomal subunit, monosome composed of one ribosome residing on mRNA and polysomes (Fig. 18).

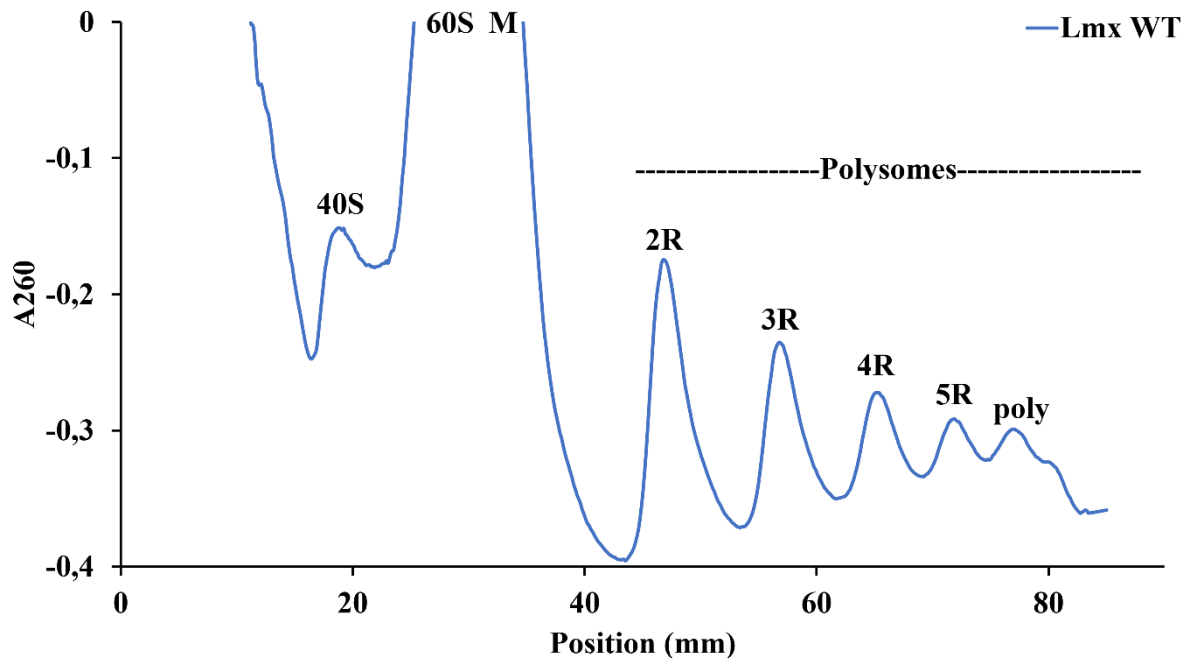


Fig. 18: Polysome analysis. Lmx WT, 1x CHX, 15x pass, 20% IGEPAL, no DTT, 5×10^6 cells/ml. 40S represents small ribosomal subunit, 60S represents large ribosomal subunit, M represents monosome. Active ribosomes (R) are separated by the amount of ribosomes bound to mRNA.

4.5.3 Polysome analysis shows a role of Q-depletion in translation

Polysome profile was performed to characterize an effect of Q depletion on translation by analysis of WT, LmxTGT2 KO, and LmxTGT2 AB cell lines. The resulting graphs show more or less similar profile of WT and LmxTGT2 AB but a significant decrease in the LmxTGT2 KO profile suggesting a specific phenotype for Q-depletion KO cell line (Fig. 19).

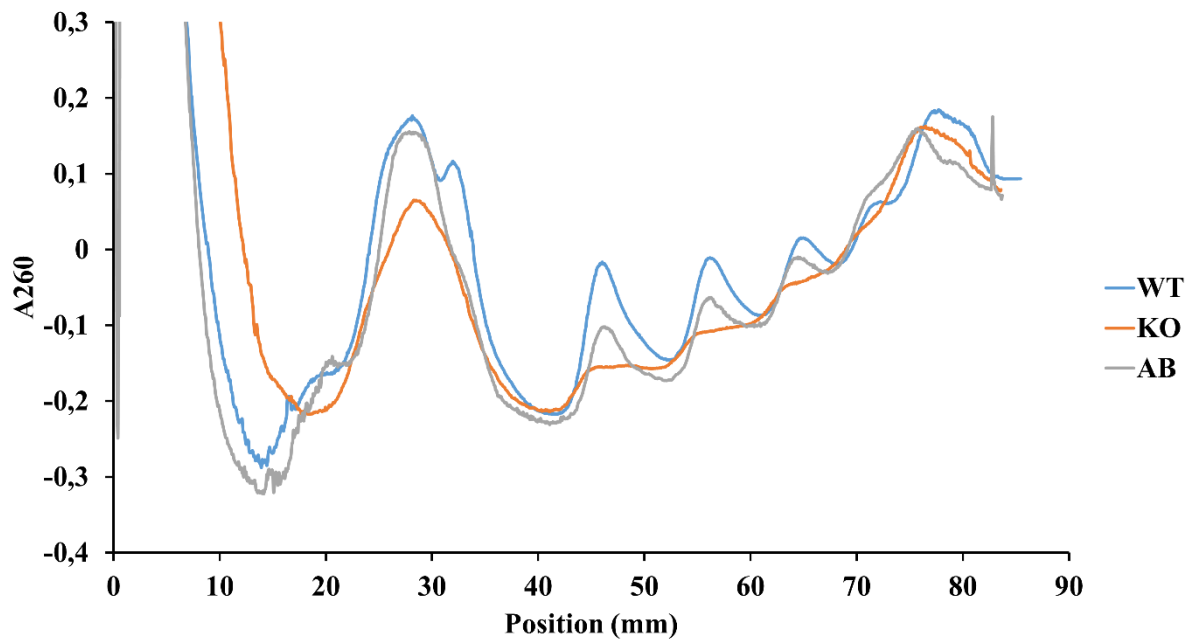


Fig. 19: Polysome analysis of WT, LmxTGT2 KO, and LmxTGT2 AB cell lines. LmxTGT2 KO cell line exhibited a different phenotype compared to WT and LmxTGT2 AB cell lines. Representative profile of multiple individual replicates.

4.5.4 Monosome density

To verify the different phenotype of TGT2 KO cell line, we normalized the highest values of the monosome peaks to the highest value of the initial peak of that cell line. The KO and AB values were further normalized to the WT cell line values. The experiment confirmed a significant difference in the monosome density in TGT2 KO (Fig. 20); thus, we can say that this is a specific phenotype due to the lack of Q modification as it is rescued by the AB construct. RNA isolated from monosome and polysome fractions of each cell line was sent in triplicate for mRNAseq, in order to identify the mRNAs most affected by the lack of Q. How this affects translation at individual codon level has to be confirmed by ribosome profiling.

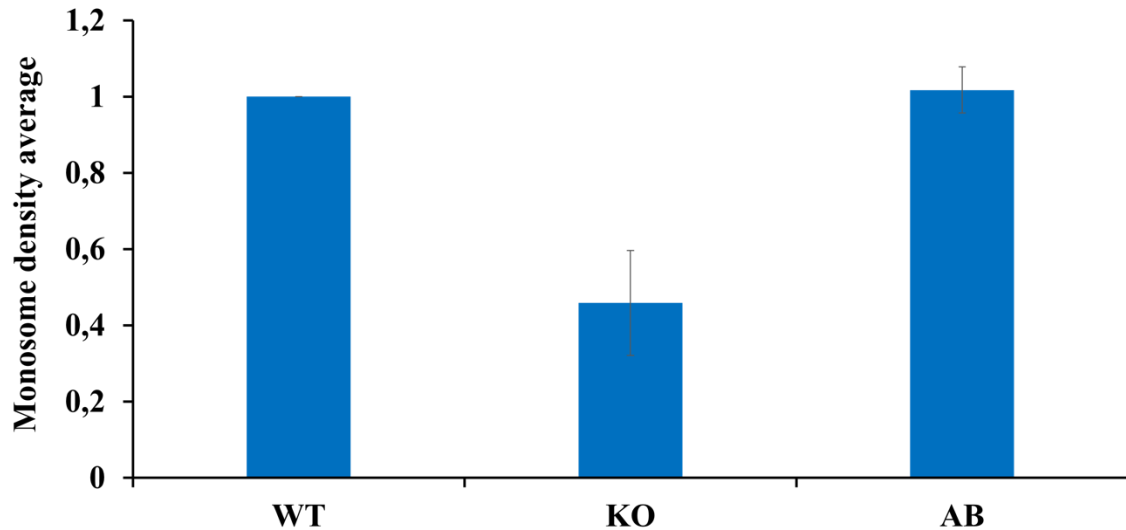


Fig. 20: Monosome density of WT, TGT2 KO and AB cell lines. Error bars represent the standard deviation of three replicates.

4.6 Ribosome profiling

4.6.1 Standardization of RNase digestion

In order to standardize the ribosome profiling protocol for *L. mexicana*, we first checked the RNase treatment by comparison with untreated control sample. Briefly, cells were lysed as described in paragraph 4.5.2, one lysate was digested with 1 600 units of RNaseI, both samples were incubated on ice for 45 min and the reaction was inhibited with 100 units of SUPERase*In. The resulting profiles were obtained as described above. The untreated sample served as a control of the technique. As a result, we are still able to see the 40S and 60S ribosomal subunits, however, the polysomes are accumulated in monosome fraction indicating that the RNase treatment was successful. In addition, we assume that the small peak next to the monosome may be formed by association of two ribosomes whose positions were so close together that RNase could not cut them (Fig. 21).

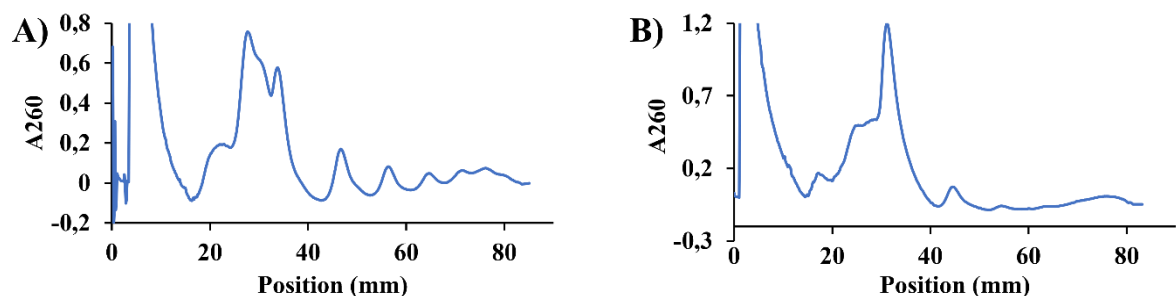


Fig. 21: Evaluation of RNase treatment. A) Lmx WT untreated; B) Lmx WT RNase treated, 1x CHX, 15x pass, 20% IGEPAL, no DTT, 5×10^6 cells/ml, 1600 units of RNase I for 45 min, 100 units of SUPERase*In.

A good hallmark of optimum RNase treatment is a balance between complete digestion of heavy polysomes, while avoiding random degradation of rRNA that leads to artifacts in the library. As we observed some heavy polysomes still undigested in the 45 min treatment, the next step in standardization was to determine whether the incubation time affected the resulting profile. We tried three different incubation times on ice, 40 minutes (Fig. 22A), 50 minutes (Fig. 22B), and 60 minutes (Fig. 22C). The experiment revealed that the sharpest peaks of both subunits and the monosome were obtained by incubation on ice for 50 minutes.

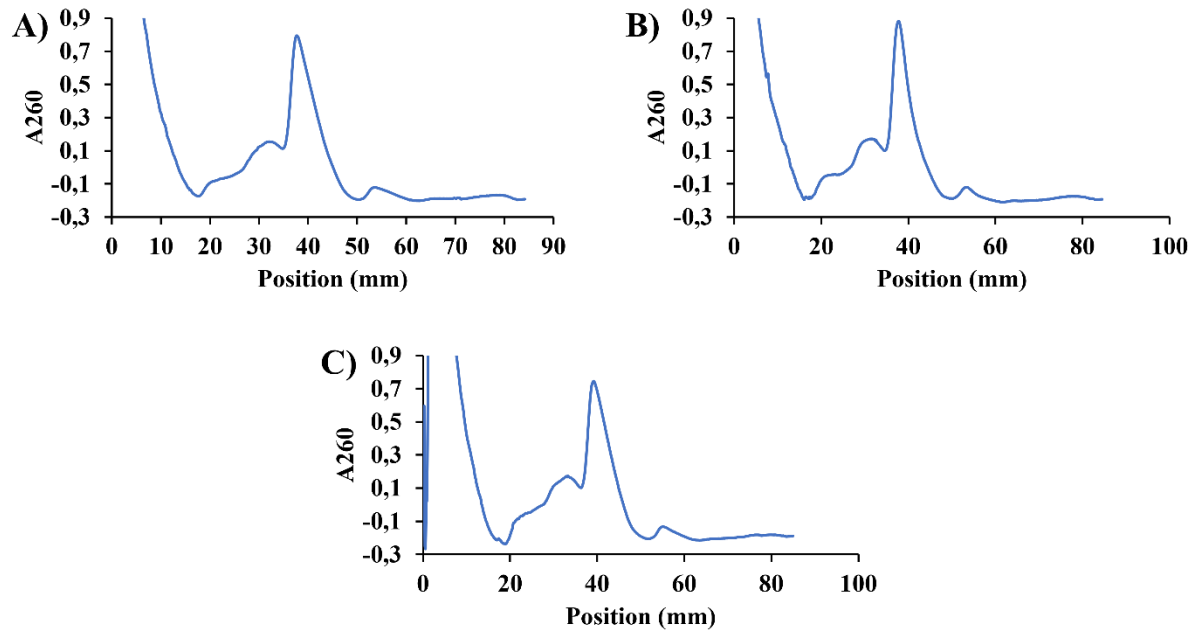


Fig. 22: RNase digestion. Lmx WT, 1x CHX, 15x pass, 20% IGEPAL, no DTT, 5×10^6 cells/ml, 1600 units of RNase I, 100 units of SUPERase*In; A) 40 min incubation; B) 50 min incubation; C) 60 min incubation.

4.6.2 Standardized profiles of RNase digestion

Using these standardized conditions, we performed the RNase digestion for all three cell lines (Fig. 23). As with the polysome profile, a different phenotype is demonstrated in the TGT2 KO profile. Even in this experiment, the values for the monosome peak of KO are lower compared to WT and AB profiles.

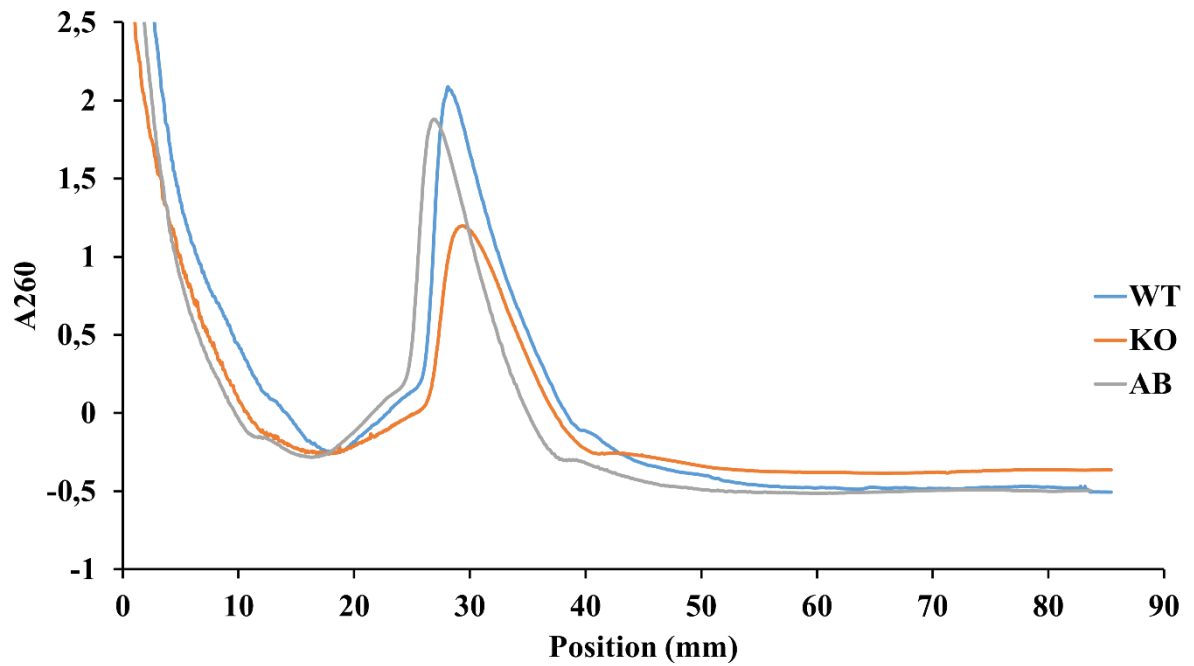


Fig. 23: RNase digestion of WT, LmxTGT2 KO, and LmxTGT2 AB cell lines. LmxTGT2 KO cell line exhibited a different phenotype compared to WT and LmxTGT2 AB cell lines. Representative profile of three individual replicates.

4.6.3 Footprint size selection

Following the RNase digestion and RNA isolation, the ribosome protected fragments (RPFs) were denatured, resolved on 15%PAA/1xNNB/8M urea gel with the control oligonucleotide marker on either side for 3 hours and stained with SYBR Gold. For each sample 26 nt – 34 nt region was excised (Fig. 24).

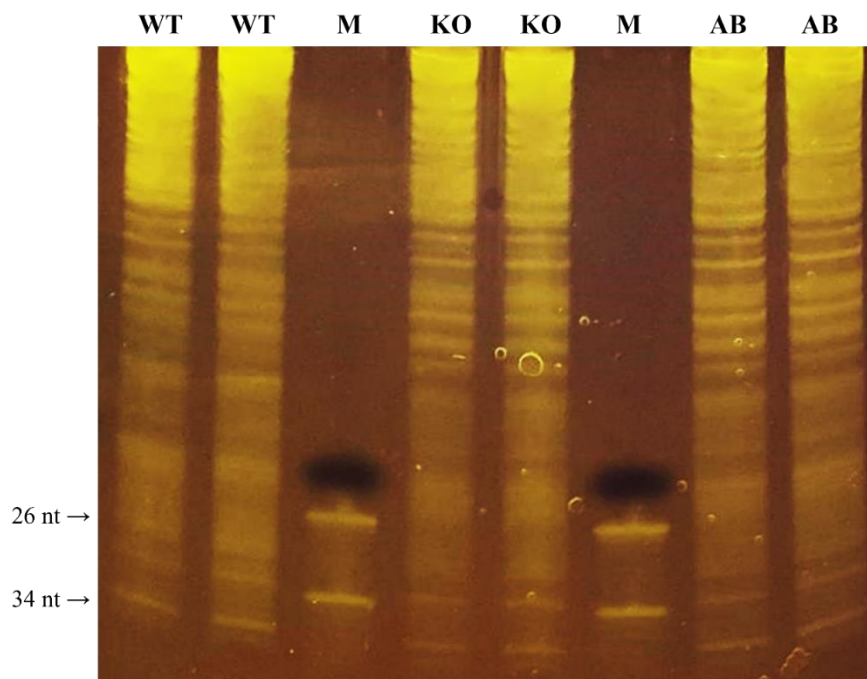


Fig. 24: Footprint size selection. RNase treated fragments were resolved on 15% NNB-Urea-polyacrylamide gel. M: oligonucleotide marker. Three biological repeats were performed, and representative gel is shown.

4.6.4 Reverse transcription

The isolated RPFs were deacylated and ligated to the linker. Oligonucleotide markers used to mark the RPF size were also treated in the same way as positive control. In order to obtain the cDNA library, the reverse transcription was performed. Following this reaction, the cDNA libraries were resolved on 10%PAA/1xNNB/8M urea gel with RT primer used as marker for 2,5 hours and stained with SYBR Gold. The region corresponding to cDNA library was excised (Fig. 25), ethanol-precipitated and resuspended in MilliQ®. Ribosome profiling libraries are often heavily contaminated with rRNA, reducing the mRNA coverage. In order to get rid of the rRNAs, biotin labeled custom oligonucleotide probes were designed in collaboration with siTOOLS Biotech GmbH. Once rRNA depletion is completed, this protocol continues with circularization of cDNA, PCR amplification and sequencing which will be finished by the summer of 2022.

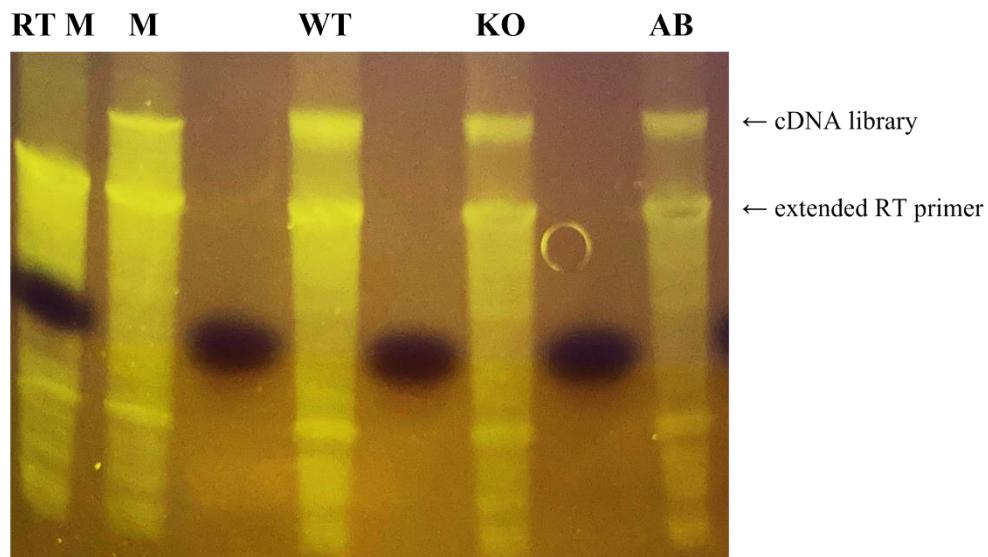


Fig. 25: Reverse transcription. cDNA libraries were resolved on 10% NNB-Urea-polyacrylamide gel. RT M: extended reverse transcription marker; M: oligonucleotide marker control library. Three biological repeats were performed, and representative gel is shown.

4.7 Lack of Q can affect the rate of protein synthesis

To test whether the Q depletion affects protein synthesis, pulse labelling with ³⁵S labeled methionine and cysteine mix was performed, the cells were resuspended in 2x Laemmli sample buffer and separated by SDS-PAGE. The gel was Coomassie-stained, dried, exposed to the Phosphoimager screen and developed for autoradiography. We hypothesized that TGT2 KO would generate less newly synthesized proteins because delays in translation.

The experiment revealed reduced radioactivity in TGT2 KO compared to WT cell line. However, this is only preliminary result which needs to be explored further, because we have not performed three biological replicates.

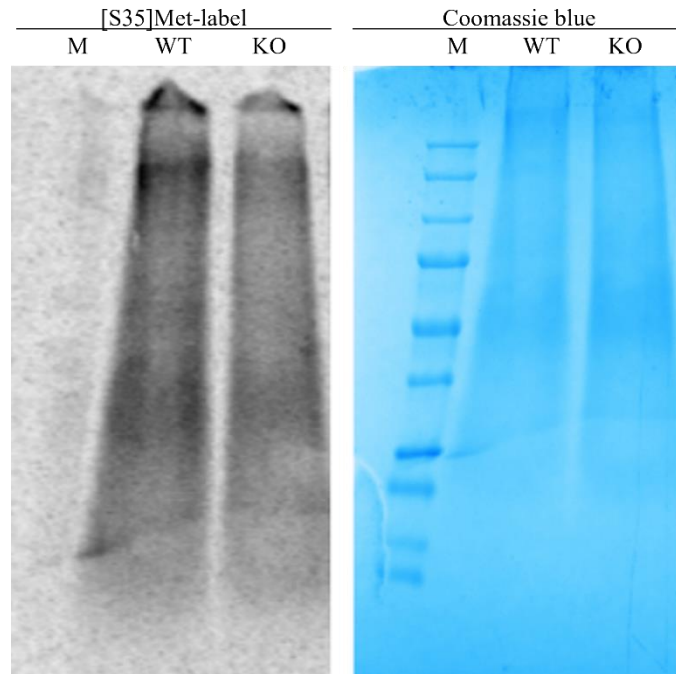


Fig. 26: Analysis of protein synthesis. The Coomassie blue used as loading control. M: size marker. Only one biological repeat was performed.

4.8 Analysis of protein aggregates

Delays in translation can cause premature termination, leading to misfolded/unfolded protein aggregates. To examine the pattern of these aggregates, cells were pulse labelled, followed by multiple sonication steps as described in the methods section. Then the samples were separated by the SDS-PAGE, Coomassie-stained, and developed for autoradiography. Although there were no visible differences in the pattern, these samples were sent for proteomics and currently, we have been analyzing the resulting data.

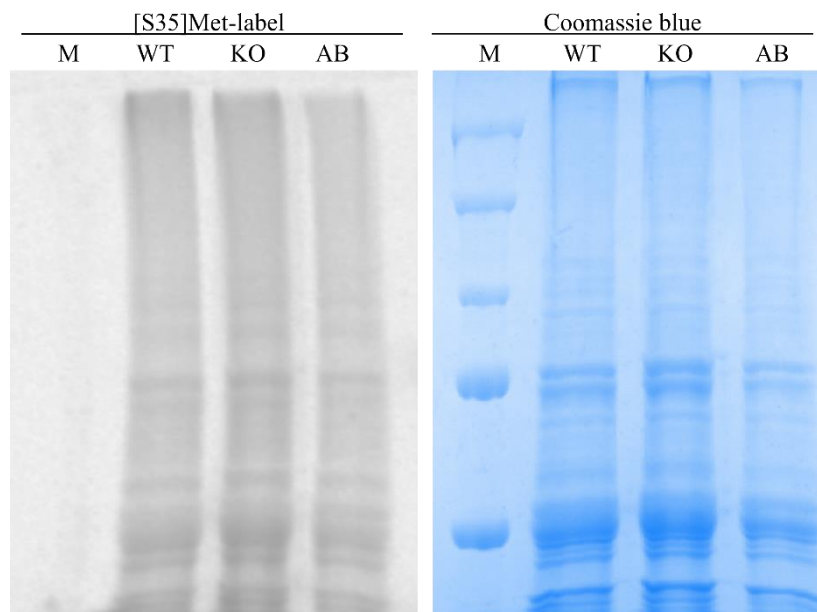


Fig. 27: Analysis of protein aggregates. The Coomassie blue used as loading control. M: size marker. Three biological repeat was performed, and representative result is shown.

5 Discussion

The aim of this project was to standardize several molecular biology techniques to study the role of Q during translation in the trypanosomatid parasite *Leishmania mexicana*. We started by confirming the cell lines used in this study for the presence/absence of Q.

5.1 The presence of Q in Lmx tRNA^{Asp, His, Tyr}

The presence of Q modification at the wobble position is reported in all domains of life with few exceptions such as *S. cerevisiae* or *C. albicans* (Kessler et al., 2018; Zallot et al., 2014). Previously, the Q modification was also demonstrated in all corresponding tRNAs in *L. mexicana* species and complete depletion of Q-tRNAs was observed in TGT2 KO cell line (Boudová, 2018). We verified the KO for the depletion of Q. In this project, we included the AB rescue cell line in our experiments. The AB construct successfully rescued the KO and restored Q modification levels to that of WT. Ideally, Q should be present in all corresponding tRNAs. However, we encountered an issue with tRNA^{Asn} and even after several repeats, we did not achieve a conclusive result which could be due to either loss of oligonucleotide functionality, or suboptimal conditions of hybridization.

5.2 The effect of Q on cell growth, life cycle and membrane potential

According to previous results from our lab (Boudová, 2018), we have some indications that Q modification plays some role in *L. mexicana* life cycle. However, these results had to be verified as they were not repeated. Thus, to confirm these results, we examined the effect of Q modification on cell growth of WT, TGT2 KO and AB strains. The resulting growth curve confirmed that Q did not affect the cell growth in culture, neither in TGT2 KO, nor in AB cell line compared to WT.

Moreover, we investigated the effect Q may have on the *L. mexicana* cell cycle. Thus, we decided to test the impact using flow cytometry. Firstly, there was some different phenotype in cell cycle of TGT2 KO as well as in AB cell line, however, we correctly assumed that this phenomenon is caused by added antibiotics (Puro and Ntc for KO medium and Puro, Ntc and Phleo for AB medium). We found this out by removing these antibiotics from media and adding only hygromycin, the essential antibiotic for the WT cell line. The graphs showed more or less similar results for all three cell lines. In addition, this experiment highlighted the importance of AB cell line in this project – if we compared only the WT and KO phenotypes in the first flow cytometry test, we might mistakenly believe that KO shows a significantly

different phenotype depending on the Q modification. However, because the similar phenotype appeared also in the AB cell line, it gave us the idea to test cells without the presence of mentioned antibiotics.

The effect of Q on the membrane potential will have to be subjected to further observation, as the result has not been verified by three biological repeats. We also need to consider that these experiments were conducted on procyclic promastigotes. The effect of Q may be more pronounced in metacyclic promastigotes or amastigotes, as indicated by other preliminary experiments in the lab.

5.3 Standardization of polysome profiling and ribosome profiling methods

There are several suggestions about the association between the tRNAs and codon usage (Ikemura, 1981) as well as that the presence of Q modification in the wobble position may affect codon usage bias (Meier et al., 1985; Morris et al., 1999; Tuorto et al., 2018). Since the codon usage bias has been reported in kinetoplastid protozoans (Alvarez et al., 1994; Neçşulea & Lobry, 2006; Parsons et al., 1991), we hypothesized that this phenomenon could also be found in *L. mexicana*. According to the Qian et al. (2012) study, in which they used the genome-wide ribosome profiling method to show that there is no difference between translation speed of preferred synonymous codons and non-preferred codons, we decided to standardize the polysome profiling protocol (Tinti et al., 2021) as well as the ribosome profiling protocol (Brar & Weissman, 2015) for *L. mexicana*.

Firstly, in the standardization experiments, we decided to passage the lysate 5 times through the needle. The resulting polysomes were not as nicely separated and did not reach such values as after 15x passages in which there was no degradation of the polysomes. Secondly, different CHX concentrations were tested. When we used 200 µg/ml, we did not observe a significant difference compared to 100 µg/ml CHX. Therefore, we decided to use the concentration recommended in the original protocol. An equally important experiment was also to test different cell densities of the input culture, which underlined the importance of using early log phase cells for optimum polysome yield. In order to test the detergents, we used three different chemicals – IGEPAL, NP₄₀, and Triton X-100. The comparison of all three results revealed that the best detergent is IGEPAL. Thus, we tried three different concentrations of IGEPAL – 10%, 20%, and 30%, when the most favorable profile was shown at a concentration of 20% due to the fact that A₂₆₀ value for polysomes gradually increased within each position on the *x*-axis. Another standardization condition for *L. mexicana* that was

chosen to perform the final experiment was incubating the culture with CHX for 5 minutes before the harvesting, as did not cause excessive degradation of the polysomes. Lastly, the samples were ultracentrifuged for 3 hours, which did not give us a positive result. In the final polysome analysis, we found that the phenotype of the TGT2 KO cell line is definitely affected. Since all final experiments were performed with cells of the same density, we can say that this phenotype is due to the lack of Q modification which causes delays during translation. Subsequently, we sent RNA isolated from monosome and polysome fractions to the sequencing. Currently, we have the data from the sequencing available; however, due to the bulk of these data, we need more time to analyze them, and thus, these results will be presented during the defense of this thesis. These results also had to be verified using ribosome profiling method, and therefore, we decided to standardize it for *L. mexicana*.

We first started by verifying whether RNase digestion would occur at all in the *L. mexicana* lysates. In the resulting profile, we are still able to see the 40S and 60S ribosomal subunits, however, the polysomes are accumulated in monosome fraction which means that the RNase treatment was successful. In addition, we assume that the small peak next to the monosome may be formed by associating of two ribosomes whose positions were so close together that RNase could not cut them. In the following experiment we found that the most suitable time for the incubation is 50 minutes, after which a significantly better profile was achieved, especially in the monosome fraction. As a result, after standardization of RNase digestion, we obtained a similar result as for the polysomes profile – monosomes in TGT2 KO are definitely affected by the lack of Q. Following the RNase digestion, we continued according to the protocol until the reverse transcription and preparation of cDNA libraries. To finish this method, cDNA circularization, PCR amplification, and sequencing are required, which will be completed in the summer of 2022.

5.4 Protein analysis

Since the codon bias is also associated in protein folding and its role has been found in mRNA and protein abundance control processes (de Freitas Nascimento et al., 2018; Jeacock et al., 2018), we decided to test the role of Q modification in protein synthesis and protein aggregates in *L. mexicana*. We hypothesized, that TGT2 KO should cause a decrease in protein synthesis as well as some difference in protein aggregates compared to WT cell line. Our preliminary experiments confirmed this hypothesis; however, this analysis needs to be repeated for statistical significance. Although the analysis of protein aggregates using SDS-PAGE did not reveal any significant difference due to Q-deficiency in TGT2 KO, a more

sensitive technique of mass spectrometry might shed more light on the effect of Q depletion on protein folding. This analysis is currently underway.

6 Conclusion

In conclusion, most of the aims of the thesis were fulfilled, contributing significantly to the overall goal of the laboratory, which is to study the function of tRNA modifications in parasitic protists. Specifically, my results may help to interpret the role of Q in parasite infection and virulence. I was able to standardize several crucial techniques for *L. mexicana*. I analyzed the role of Q modification in the cell cycle of *L. mexicana* using flow cytometry. Additionally, I standardized the polysome profiling method. My results suggest that the translation of LmxTGT2 KO cell line is affected by the lack of queuosine. I believe that this will be supported in the future by ribosome profiling, which I have established in the laboratory. I also investigated the effect of Q on protein synthesis. I generated several high-throughput datasets during this project, which will need further exploration. Combining the sequencing data from polysome and ribosome profiling with the proteomics data will undoubtedly complete the puzzle of the role Q during translation in *L. mexicana*.

7 Appendix

7.1 Annex 1 – Common buffers

a) 10% formalin solution

Components
3,6% formaldehyde
150 mM NaCl
15 mM $\text{Na}_3\text{C}_6\text{H}_5\text{O}_7$

b) PBS buffer

Components
137 mM NaCl
2,7 mM KCl
10 mM Na_2HPO_4
1,8 mM KH_2PO_4

c) Solution D

Components
4 M guanidine isothiocyanate
25 mM sodium citrate (pH 7.0)
0,5% sarcosyl
0,1 M β -mercaptoethanol

d) PDC buffer

Components
10 mM Tris-HCl (pH 7.4)
300 mM KCl
10 mM MgCl_2

e) 1x NNB

Components
89 mM Tris base $\text{NH}_2\text{C}(\text{CH}_2\text{OH})_3$
89 mM boric acid
2 mM EDTA

f) RNA gel loading buffer

Components
Formamide
10x NNB
20% SDS
<i>With dye:</i>
0,03% xylene cyanol
0,03% bromophenol blue

g) Gel elution buffer

Components
0,3 M NaOAc (pH 5.2)
1 mM EDTA (pH 8.0)
0,1 U/ μl SUPERase*In

h) PI solution

Components
1x PBS
10 $\mu\text{l}/\text{ml}$ PI
9,6 $\mu\text{g}/\text{ml}$ RNase A
0,2% Triton X100

7.2 Annex 2 – Northern blotting and oligonucleotide hybridization buffers

a) Urea loading dye

Components
8 M urea
20 mM Tris-HCl (pH 8.0)
1 mM EDTA

b) 50x TAE

Components
2M Tris base
1M glacial acetic acid
50mM EDTA

c) Hybridization solution

Components
5x SSC
20 mM P ₁ (pH 7.0)
7% SDS
1 mg/ml salmon sperm DNA
1x Denhardt's solution

d) Denhardt's solution

Components
0,02% Ficoll 400
0,02% polyvinylpyrrolidone
0,02% bovine serum albumine (BSA)

e) Wash buffer 1

Components
3x SSC
5% SDS
25 mM NaH ₂ PO ₄ (pH 7.5)
10x Denhardt's solution

f) Wash buffer 2

Components
1x SSC
1% SDS

g) Stripping solution

Components
0,1% SSC
0,1% SDS

7.3 Annex 3 – Proteomics buffers

a) Lysis buffer

Components
20 mM Na-phosphate (pH 6.8)
10 mM DTT
1 mM EDTA
0,1% Tween 20
Protease inhibitor cocktail

b) Protein aggregates wash buffer

Components
20 mM Na-phosphate (pH 6.8)
2% NP-40
Protease inhibitor cocktail

7.4 Annex 4 – Oligonucleotide sequences

a) Oligonucleotides used for hybridization

Probe	5'-3' sequence
tRNA ^{Asn}	CCTCCCGTTGGATTCGAAC
tRNA ^{Asp}	TCCCGGCCGGGAATTGAA
tRNA ^{His}	GGGGAAACCGGGAATCGGAC
tRNA ^{Tyr}	CCTTCCGGCCGGGAATTCGAAC
tRNA ^{Ile}	CCAACAGGGGTCTGAACCTGTGACC

b) Markers

Marker	5'-3' sequence
RNA con 26 nt	AUGUACACGGAGUCGACCCAACGCGA-(Phos)
RNA con 34 nt	AUGUACACGGAGUCGAGCUCAACCCGCAACGCGA-(Phos)

c) RT primer

5'-(Phos)-AGATCGGAAGAGCGTCGTGTAGGGAAAGAGTGTAGATCTCGGTGGTCC
C-(SpC18)-CACTCA-(SpC18)-TTCAGACGTGTGCTCTTCCGATCTATTGATGGTGCC
TACAG-3'

7.5 Annex 5 – RNA gel solutions

a) 15%PAA/1xNNB/8M urea gel

Total volume	20 ml	35 ml
Components	Volume	Volume
10x NNB	2 ml	3,5 ml
Acrylamide 40% (19:1)	7,5 ml	13,1 ml
Urea 8M	9,6 g	16,8 g
APS	180 µl	180 µl
TEMED	18 µl	18 µl

b) 10%PAA/1xNNB/8M urea gel

Total volume	20 ml	35 ml
Components	Volume	Volume
10x NNB	2 ml	3,5 ml
Acrylamide 40% (19:1)	5 ml	8,8 ml
Urea 8M	9,6 g	16,8 g
APS	180 µl	180 µl
TEMED	18 µl	18 µl

8 List of references

- Akhoundi, M., Kuhls, K., Cannet, A., Votýpka, J., Marty, P., Delaunay, P., & Sereno, D. (2016). A historical overview of the classification, evolution, and dispersion of *Leishmania* parasites and sandflies. *PLOS Neglected Tropical Diseases*, *10*(3).
- Alvarez, F., Robello, C., Vignali, M., Robeilo, C., & Vignalp, M. (1994). Evolution of codon usage and base contents in kinetoplastid protozoans. *Molecular Biology and Evolution*, *11*(5), 790–802.
- Anderson, P., & Ivanov, P. (2014). tRNA fragments in human health and disease. *FEBS Letters*, *588*(23), 4297–4304.
- Arava, Y., Wang, Y., Storey, J. D., Liu, C. L., Brown, P. O., & Herschlag, D. (2003). Genome-wide analysis of mRNA translation profiles in *Saccharomyces cerevisiae*. *Proceedings of the National Academy of Sciences*, *100*(7), 3889–3894.
- Aslett, M., Aurrecochea, C., Berriman, M., Brestelli, J., Brunk, B. P., Carrington, M., Depledge, D. P., Fischer, S., Gajria, B., Gao, X., Gardner, M. J., Gingle, A., Grant, G., Harb, O. S., Heiges, M., Hertz-Fowler, C., Houston, R., Innamorato, F., Iodice, J., Wang, H. (2010). TriTrypDB: a functional genomic resource for the Trypanosomatidae. *Nucleic Acids Research*, *38*, D457–D462.
- Attardi, G. (1967). The mechanism of protein synthesis. *Annual Review of Microbiology*, *21*(1), 383–416.
- Behura, S. K., & Severson, D. W. (2013). Codon usage bias: causative factors, quantification methods and genome-wide patterns: with emphasis on insect genomes. *Biological Reviews*, *88*(1), 49–61.
- Berg, M. D., Giguere, D. J., Dron, J. S., Lant, J. T., Genereaux, J., Liao, C., Wang, J., Robinson, J. F., Gloor, G. B., Hegele, R. A., O'Donoghue, P., & Brandl, C. J. (2019). Targeted sequencing reveals expanded genetic diversity of human transfer RNAs. *RNA Biology*, *16*(11), 1574–1585.
- Biela, I., Tidten-Luksch, N., Immekus, F., Glinca, S., Nguyen, T. X. P., Gerber, H.-D., Heine, A., Klebe, G., & Reuter, K. (2013). Investigation of specificity determinants in bacterial tRNA-guanine transglycosylase reveals queuine, the substrate of its eucaryotic counterpart, as inhibitor. *PLoS ONE*, *8*(5).
- Boudová Michala. (2018). The role of Q tRNA modification in the virulence of *Leishmania mexicana*.

- Brar, G. A., & Weissman, J. S. (2015). Ribosome profiling reveals the what, when, where and how of protein synthesis. *Nature Reviews Molecular Cell Biology*, *16*(11), 651–664.
- CDC (2020). Parasites – Leishmaniasis.
- Chen, Y.-C., Kelly, V. P., Stachura, S. v., & Garcia, G. A. (2010). Characterization of the human tRNA-guanine transglycosylase: Confirmation of the heterodimeric subunit structure. *RNA*, *16*(5), 958–968.
- Chomczynski, P., & Sacchi, N. (2006). The single-step method of RNA isolation by acid guanidinium thiocyanate–phenol–chloroform extraction: twenty-something years on. *Nature Protocols*, *1*(2), 581–585.
- Cortazzo, P., Cerveñansky, C., Martín, M., Reiss, C., Ehrlich, R., & Deana, A. (2002). Silent mutations affect in vivo protein folding in *Escherichia coli*. *Biochemical and Biophysical Research Communications*, *293*(1), 537–541.
- Christie, N. T., Owenby, R. K., Jacobson, K. B., Hiatt, V. S., & Farkas, W. R. (1982). Queuine-containing isoacceptor of tyrosine tRNA in *Drosophila melanogaster*. *Biochimica et Biophysica Acta (BBA) - Gene Structure and Expression*, *699*(1), 40–48.
- Crick, F. H. C. (1966). Codon—anticodon pairing: The wobble hypothesis. *Journal of Molecular Biology*, *19*(2), 548–555.
- Crowley, L. C., Christensen, M. E., & Waterhouse, N. J. (2016). Measuring mitochondrial transmembrane potential by TMRE staining. *Cold Spring Harbor Protocols*, *2016*(12).
- de Freitas Nascimento, J., Kelly, S., Sunter, J., & Carrington, M. (2018). Codon choice directs constitutive mRNA levels in trypanosomes. *ELife*, *7*.
- de Vries, H. J. C., Reedijk, S. H., & Schallig, H. D. F. H. (2015). Cutaneous leishmaniasis: recent developments in diagnosis and management. *American Journal of Clinical Dermatology*, *16*(2), 99–109.
- DeCaprio, J., & Kohl, T. O. (2018). Pulse-chase labeling of protein antigens with [³⁵S]methionine. *Cold Spring Harbor Protocols*, *2018*(9).
- Dixit, S., Kessler, A. C., Henderson, J., Pan, X., Zhao, R., D’Almeida, G. S., Kulkarni, S., Rubio, M. A. T., Hegedúsová, E., Ross, R. L., Limbach, P. A., Green, B. D., Paris, Z., & Alfonzo, J. D. (2021). Dynamic queuosine changes in tRNA couple nutrient levels to codon choice in *Trypanosoma brucei*. *Nucleic Acids Research*, *49*(22), 12986–12999.

- Dong, H., Nilsson, L., & Kurland, C. G. (1996). Co-variation of tRNA abundance and codon usage in *Escherichia coli* at different growth rates. *Journal of Molecular Biology*, 260(5), 649–663.
- Duret, L. (2002). Evolution of synonymous codon usage in metazoans. *Current Opinion in Genetics and Development, Elsevier Ltd.*, 12(6), 640 – 649.
- Duret, L., & Mouchiroud, D. (1999). Expression pattern and, surprisingly, gene length shape codon usage in *Caenorhabditis*, *Drosophila*, and *Arabidopsis*. *Proceedings of the National Academy of Sciences*, 96(8), 4482–4487.
- Fenn, K., & Matthews, K. R. (2007). The cell biology of *Trypanosoma brucei* differentiation. *Current Opinion in Microbiology*, 10(6), 539–546.
- Fergus, C., Barnes, D., Alqasem, M., & Kelly, V. (2015). The queuine micronutrient: charting a course from microbe to man. *Nutrients*, 7(4), 2897–2929.
- Gaur, R., Björk, G. R., Tuck, S., & Varshney, U. (2007). Diet-dependent depletion of queuosine in tRNAs in *Caenorhabditis elegans* does not lead to a developmental block. *Journal of Biosciences*, 32(4), 747–754.
- Gonzalez, D. L., Giannerini, S., & Rosa, R. (2019). On the origin of degeneracy in the genetic code. *Interface Focus*, 9(6), 20190038.
- Gossage, S. M., Rogers, M. E., & Bates, P. A. (2003). Two separate growth phases during the development of *Leishmania* in sand flies: implications for understanding the life cycle. *International Journal for Parasitology*, 33(10), 1027–1034.
- Grantham, R. (1980). Working of the genetic code. *Trends in Biochemical Sciences*, 5(12), 327–331.
- Grantham, R., Gautier, C., Gouy, M., Jacobzone, M., & Mercier, R. (1981). Codon catalog usage is a genome strategy modulated for gene expressivity. *Nucleic Acids Research*, 9(1), 213–213.
- Hanson, G., & Collier, J. (2018). Codon optimality, bias and usage in translation and mRNA decay. *Nature Reviews Molecular Cell Biology*, 19(1), 20–30.
- Heaphy, S.M., Mariotti, M., Gladyshev, V.N., Atkins, J.F., Baranov, P. V. (2016). Novel ciliate genetic code variants including the reassignment of all three stop codons to sense codons in *Condylostoma magnum*. *Molecular Biology and Evolution*, 33, 2885–2889.
- Higgs, P. G., & Ran, W. (2008). Coevolution of codon usage and tRNA genes leads to alternative stable states of biased codon usage. *Molecular Biology and Evolution*, 25(11), 2279–2291.

- Igloi, G. L., & Kössel, H. (1985). Affinity electrophoresis for monitoring terminal phosphorylation and the presence of queuosine in RNA. Application of polyacrylamide containing a covalently bound boronic acid. *Nucleic Acids Research*, *13*(19), 6881–6898.
- Ikemura, T. (1981). Correlation between the abundance of *Escherichia coli* transfer RNAs and the occurrence of the respective codons in its protein genes: A proposal for a synonymous codon choice that is optimal for the *E. coli* translational system. *Journal of Molecular Biology*, *151*(3), 389–409.
- Ingolia, N. T., Ghaemmaghami, S., Newman, J. R. S., & Weissman, J. S. (2009). Genome-wide analysis in vivo of translation with nucleotide resolution using ribosome profiling. *Science*, *324*(5924), 218–223.
- Ishiwata, S., Katayama, J., Shindo, H., Ozawa, Y., Itoh, K., & Mizugaki, M. (2001). Increased expression of queuosine synthesizing enzyme, tRNA-guanine transglycosylase, and queuosine levels in tRNA of leukemic cells. *Journal of Biochemistry*, *129*(1), 13–17.
- Jeacock, L., Faria, J., & Horn, D. (2018). Codon usage bias controls mRNA and protein abundance in trypanosomatids. *ELife*, *7*.
- Kanaya, S., Yamada, Y., Kinouchi, M., Kudo, Y., & Ikemura, T. (2001). Codon usage and tRNA genes in eukaryotes: correlation of codon usage diversity with translation efficiency and with CG-dinucleotide usage as assessed by multivariate analysis. *Journal of Molecular Evolution*, *53*(4–5), 290–298.
- Karamysheva, Z. N., Gutierrez Guarnizo, S. A., & Karamyshev, A. L. (2020). Regulation of translation in the protozoan parasite *Leishmania*. *International Journal of Molecular Sciences*, *21*(8), 2981.
- Katze, J. R., & Beck, W. T. (1980). Administration of queuine to mice relieves modified nucleoside queuosine deficiency in Ehrlich ascites tumor tRNA. *Biochemical and Biophysical Research Communications*, *96*(1), 313–319.
- Kessler, A. C., Kulkarni, S. S., Paulines, M. J., Rubio, M. A. T., Limbach, P. A., Paris, Z., & Alfonzo, J. D. (2018). Retrograde nuclear transport from the cytoplasm is required for tRNA^{Tyr} maturation in *T. brucei*. *RNA Biology*, *15*(4–5), 528–536.
- Kessler, A. C., Silveira d’Almeida, G., & Alfonzo, J. D. (2018). The role of intracellular compartmentalization on tRNA processing and modification. *RNA Biology*, *15*(4–5), 554–566.

- Kim, J., Klein, P. G., & Mullet, J. E. (1991). Ribosomes pause at specific sites during synthesis of membrane-bound chloroplast reaction center protein D1. *Journal of Biological Chemistry*, 266(23), 14931–14938.
- King, R. C., Stansfield, W. D., & Mulligan, P. K. (2007). *A Dictionary of Genetics*. Oxford University Press.
- Kirtland, G. M., Morris, T. D., Moore, P. H., O'Brian, J. J., Edmonds, C. G., McCloskey, J. A., & Katze, J. R. (1988). Novel salvage of queuine from queuosine and absence of queuine synthesis in *Chlorella pyrenoidosa* and *Chlamydomonas reinhardtii*. *Journal of Bacteriology*, 170(12), 5633–5641.
- Klepper, F., Jahn, E.-M., Hickmann, V., & Carell, T. (2007). Synthesis of the transfer-RNA nucleoside queuosine by using a chiral allyl azide intermediate. *Angewandte Chemie International Edition*, 46(13), 2325–2327.
- Koplin, A., Preissler, S., Ilina, Y., Koch, M., Scior, A., Erhardt, M., & Deuerling, E. (2010). A dual function for chaperones SSB–RAC and the NAC nascent polypeptide-associated complex on ribosomes. *Journal of Cell Biology*, 189(1), 57–68.
- Kulkarni, S. (2021). Role of queuosine tRNA modification in the parasitic protist *Trypanosoma brucei*.
- Kulkarni, S., Rubio, M. A. T., Hegedúsová, E., Ross, R. L., Limbach, P. A., Alfonzo, J. D., & Paris, Z. (2021). Preferential import of queuosine-modified tRNAs into *Trypanosoma brucei* mitochondrion is critical for organellar protein synthesis. *Nucleic Acids Research*, 49(14), 8247–8260.
- LeBowitz, J. H., Smith, H. Q., Rusche, L., & Beverley, S. M. (1993). Coupling of poly(A) site selection and trans-splicing in *Leishmania*. *Genes & Development*, 7(6), 996–1007.
- Lorenz, C., Lünse, C., & Mörl, M. (2017). tRNA modifications: impact on structure and thermal adaptation. *Biomolecules*, 7(4), 35.
- Luzak, V., López-Escobar, L., Siegel, T. N., & Figueiredo, L. M. (2021). Cell-to-cell heterogeneity in trypanosomes. *Annual Review of Microbiology*, 75(1), 107–128.
- Marks, T., & Farkas, W. R. (1997). Effects of a diet deficient in tyrosine and queuine on germfree mice. *Biochemical and Biophysical Research Communications*, 230(2), 233–237.
- McDonagh, P. D. (2000). The unusual gene organization of *Leishmania major* chromosome 1 may reflect novel transcription processes. *Nucleic Acids Research*, 28(14), 2800–2803.

- McGwire, B. S., & Satoskar, A. R. (2014). Leishmaniasis: clinical syndromes and treatment. *QJM*, *107*(1), 7–14.
- Meier, F., Suter, B., Grosjean, H., Keith, G., & Kubli, E. (1985). Queuosine modification of the wobble base in tRNA^{His} influences “*in vivo*” decoding properties. *The EMBO Journal*, *4*(3), 823–827.
- Morris, R. C., Brown, K. G., & Elliott, M. S. (1999). The effect of queuosine on tRNA structure and function. *Journal of Biomolecular Structure & Dynamics*, *16*(4), 757–774.
- Neçşulea, A., & Lobry, J. R. (2006). Revisiting the directional mutation pressure theory: the analysis of a particular genomic structure in *Leishmania major*. *Gene*, *385*, 28–40.
- Nedialkova, D. D., & Leidel, S. A. (2015). Optimization of codon translation rates via tRNA modifications maintains proteome integrity. *Cell*, *161*(7), 1606–1618.
- Novoa, E. M., Pavon-Eternod, M., Pan, T., & Ribas De Pouplana, L. (2012). A role for tRNA modifications in genome structure and codon usage. *Cell*, *149*(1), 202–213.
- Novoa, E. M., & Ribas de Pouplana, L. (2012). Speeding with control: codon usage, tRNAs, and ribosomes. *Trends in Genetics*, *28*(11), 574–581.
- Ouellette, R. J., & Rawn, J. D. (2018). Nucleosides, nucleotides, and nucleic acids. In *Organic Chemistry* (pp. 973–1000). Elsevier.
- Paris, Z., Fleming, I. M. C., & Alfonzo, J. D. (2012). Determinants of tRNA editing and modification: Avoiding conundrums, affecting function. *Seminars in Cell & Developmental Biology*, *23*(3), 269–274.
- Parsons, M., Stuart, K., & Smiley, B. L. (1991). *Trypanosoma brucei*: Analysis of codon usage and nucleotide composition of nuclear genes. *Experimental Parasitology*, *73*(1), 101–105.
- Phillips, G., & de Crécy-Lagard, V. (2011). Biosynthesis and function of tRNA modifications in Archaea. *Current Opinion in Microbiology*, *14*(3), 335–341.
- Phizicky, E. M., & Hopper, A. K. (2015). tRNA processing, modification, and subcellular dynamics: past, present, and future. *RNA*, *21*(4), 483–485.
- Qian, W., Yang, J. R., Pearson, N. M., Maclean, C., & Zhang, J. (2012). Balanced codon usage optimizes eukaryotic translational efficiency. *PLoS Genetics*, *8*(3).
- Rakovich, T., Boland, C., Bernstein, I., Chikwana, V. M., Iwata-Reuyl, D., & Kelly, V. P. (2011). Queuosine deficiency in eukaryotes compromises tyrosine production

through increased tetrahydrobiopterin oxidation. *Journal of Biological Chemistry*, 286(22), 19354–19363.

- Ramalho-Ortigao, M. (2010). Sand fly-*Leishmania* interactions: long relationships are not necessarily easy. *The Open Parasitology Journal*, 4(1), 195–204.
- Randerath, E., Agrawal, H. P., & Randerath, K. (1984). Specific lack of the hypermodified nucleoside, queuosine, in hepatoma mitochondrial aspartate transfer RNA and its possible biological significance. *Cancer Research*, 44(3), 1167–1171.
- Reis, M. d. (2004). Solving the riddle of codon usage preferences: a test for translational selection. *Nucleic Acids Research*, 32(17), 5036–5044.
- Reyniers, J. P., Pleasants, J. R., Wostmann, B. S., Katze, J. R., & Farkas, W. R. (1981). Administration of exogenous queuine is essential for the biosynthesis of the queuosine-containing transfer RNAs in the mouse. *The Journal of Biological Chemistry*, 256(22), 11591–11594.
- Riccardi, C., & Nicoletti, I. (2006). Analysis of apoptosis by propidium iodide staining and flow cytometry. *Nature Protocols*, 1(3), 1458–1461.
- Rogers, M. B., Hilley, J. D., Dickens, N. J., Wilkes, J., Bates, P. A., Depledge, D. P., Harris, D., Her, Y., Herzyk, P., Imamura, H., Otto, T. D., Sanders, M., Seeger, K., Dujardin, J.-C., Berriman, M., Smith, D. F., Hertz-Fowler, C., & Mottram, J. C. (2011). Chromosome and gene copy number variation allow major structural change between species and strains of *Leishmania*. *Genome Research*, 21(12), 2129–2142.
- Romier, C., Reuter, K., Suck, D., & Ficner, R. (1996). Crystal structure of tRNA-guanine transglycosylase: RNA modification by base exchange. *The EMBO Journal*, 15(11), 2850–2857.
- Sacks, D., & Kamhawi, S. (2001). Molecular aspects of parasite-vector and vector-host interactions in leishmaniasis. *Annual Review of Microbiology*, 55(1), 453–483.
- Saunders, R., & Deane, C. M. (2010). Synonymous codon usage influences the local protein structure observed. *Nucleic Acids Research*, 38(19), 6719–6728.
- Schachner, E., Aschhoff, H.-J., & Kersten, H. (1984). Specific changes in lactate levels, lactate dehydrogenase patterns and cytochrome b559 in *Dictyostelium discoideum* caused by queuine. *European Journal of Biochemistry*, 139(3), 481–487.
- Schachner, E., & Kersten, H. (1984). Queuine deficiency and restoration in *Dictyostelium discoideum* and related early developmental changes. *Microbiology*, 130(1), 135–144.

- Schaffer, A. E., Pinkard, O., & Collier, J. M. (2019). tRNA metabolism and neurodevelopmental disorders. *Annual Review of Genomics and Human Genetics*, 20(1), 359–387.
- Shapira, M., Zilka, A., Garlapati, S., Dahan, E., Dahan, I., & Yavesky, V. (2001). Post transcriptional control of gene expression in *Leishmania*. *Medical Microbiology and Immunology*, 190(1–2), 23–26.
- Siard, T. J., Jacobson, K. B., & Farkas, W. R. (1991). Queuine metabolism and cadmium toxicity in *Drosophila melanogaster*. *BioFactors (Oxford, England)*, 3(1), 41–47.
- Simpson, A. M., Suyama, Y., Dewcs, H., Campbell, D. A., & Simpson, L. (1989). Kinetoplastid mitochondria contain functional tRNAs which are encoded in nuclear DNA and also contain small minicircle and maxicircle transcripts of unknown function. *Nucleic Acids Research*, 17(14), 5427–5446.
- Singhal, R. P., Kopper, R. A., Nishimura, S., & Shindo-Okada, N. (1981). Modification of guanine to queuine in transfer RNAs during development and aging. *Biochemical and Biophysical Research Communications*, 99(1), 120–126.
- Sunter, J., & Gull, K. (2017). Shape, form, function and *Leishmania* pathogenicity: from textbook descriptions to biological understanding. *Open Biology*, 7(9), 170165.
- Swart, E.C., Serra, V., Petroni, G., Nowacki, M. (2016). Genetic codes with no dedicated stop codon context-dependent translation termination. *Cell*, 166, 691–702.
- Taslimi, Y., Zahedifard, F., & Rafati, S. (2018). Leishmaniasis and various immunotherapeutic approaches. *Parasitology*, 145(4), 497–507.
- Tinti, M., Kelner-Mirôn, A., Marriott, L. J., & Ferguson, M. A. J. (2021). Polysomal mRNA association and gene expression in *Trypanosoma brucei*. *Wellcome Open Research*, 6, 36.
- Torres-Guerrero, E., Quintanilla-Cedillo, M. R., Ruiz-Esmenjaud, J., & Arenas, R. (2017). Leishmaniasis: a review. *F1000Research*, 6, 750.
- Tuller, T., Carmi, A., Vestsigian, K., Navon, S., Dorfan, Y., Zaborske, J., Pan, T., Dahan, O., Furman, I., & Pilpel, Y. (2010). An evolutionarily conserved mechanism for controlling the efficiency of protein translation. *Cell*, 141(2), 344–354.
- Tuorto, F., Legrand, C., Cirzi, C., Federico, G., Liebers, R., Müller, M., Ehrenhofer-Murray, A. E., Dittmar, G., Gröne, H., & Lyko, F. (2018). Queuosine-modified tRNAs confer nutritional control of protein translation. *The EMBO Journal*, 37(18).

- Tuorto, F., & Lyko, F. (2016). Genome recoding by tRNA modifications. *Open Biology*, 6(12), 160287.
- Ullu, E., Matthews, K. R., & Tschudi, C. (1993). Temporal order of RNA-processing reactions in trypanosomes: rapid trans splicing precedes polyadenylation of newly synthesized tubulin transcripts. *Molecular and Cellular Biology*, 13(1), 720–725.
- Vandenberg, D. J., Grant, M. D., & Severns, V. (2003). A simple tandem repeat polymorphism is present in the eighth intron of FLJ12960, a possible queuine salvage enzyme gene. *Molecular and Cellular Probes*, 17(6), 319–320.
- Varghese, S., Cotter, M., Chevot, F., Fergus, C., Cunningham, C., Mills, K. H., Connon, S. J., Southern, J. M., & Kelly, V. P. (2016). *In vivo* modification of tRNA with an artificial nucleobase leads to full disease remission in an animal model of multiple sclerosis. *Nucleic Acids Research*, gkw847.
- Vinayak, M., & Pathak, C. (2010). Queuosine modification of tRNA: its divergent role in cellular machinery. *Bioscience Reports*, 30(2), 135–148.
- Wang, D., & Farhana, A. (2022). *Biochemistry, RNA Structure*.
- WHO (2021). Leishmaniasis fact sheet. Geneva: World Health Organization; 2021.
- WHO (2020). Status of endemicity of cutaneous leishmaniasis worldwide, 2020.
- Yanagitani, K., Kimata, Y., Kadokura, H., & Kohno, K. (2011). Translational pausing ensures membrane targeting and cytoplasmic splicing of XBP1u mRNA. *Science*, 331(6017), 586–589.
- Yuan, Y., Zallot, R., Grove, T. L., Payan, D. J., Martin-Verstraete, I., Šepić, S., Balamkundu, S., Neelakandan, R., Gadi, V. K., Liu, C.-F., Swairjo, M. A., Dedon, P. C., Almo, S. C., Gerlt, J. A., & de Crécy-Lagard, V. (2019). Discovery of novel bacterial queuine salvage enzymes and pathways in human pathogens. *Proceedings of the National Academy of Sciences*, 116(38), 19126–19135.
- Záhonová, K., Kostygov, A.Y., Ševčíková, T., Yurchenko, V., Eliáš, M. (2016). An unprecedented non-canonical nuclear genetic code with all three termination codons reassigned as sense codons. *Current Biology*, 26, 2364–2369.
- Zallot, R., Brochier-Armanet, C., Gaston, K. W., Forouhar, F., Limbach, P. A., Hunt, J. F., & de Crécy-Lagard, V. (2014). Plant, animal, and fungal micronutrient queuosine is salvaged by members of the DUF2419 protein family. *ACS Chemical Biology*, 9(8), 1812–1825.